Environmental Science Nano

ROYAL SOCIETY OF CHEMISTRY

PAPER

View Article Online
View Journal | View Issue

Check for updates

Cite this: *Environ. Sci.: Nano*, 2022, **9**, 2922

Metabolic alterations in alga *Chlamydomonas reinhardtii* exposed to $nTiO_2$ materials†

Wei Liu, [a] Mengting Li,[a] Weiwei Li,[b] Arturo A. Keller [b] and Vera I. Slaveykova *[a]

Nano-sized titanium dioxide ($nTiO_2$) is one of the most commonly used materials, however the knowledge about the molecular basis for metabolic and physiological changes in phytoplankton is yet to be explored. In the present study we use a combination of targeted metabolomics, transcriptomics and physiological response studies to decipher the metabolic perturbation in green alga *Chlamydomonas reinhardtii* exposed for 72 h to increasing concentrations (2, 20, 100 and 200 mg L^{-1}) of $nTiO_2$ with primary sizes of 5, 15 and 20 nm. Results show that the exposure to all three $nTiO_2$ materials induced perturbation of the metabolism of amino acids, nucleotides, fatty acids, tricarboxylic acids, antioxidants but not in the photosynthesis. The alterations of the most responsive metabolites were concentration and primary size-dependent despite the significant formation of micrometer-size aggregates and their sedimentation. The metabolic perturbations corroborate the observed physiological responses and transcriptomic results and confirmed the importance of oxidative stress as a major toxicity mechanism for $nTiO_2$. Transcriptomics revealed also an important influence of $nTiO_2$ treatments on the transport, adenosine triphosphate binding cassette transporters, and metal transporters, suggesting a perturbation in a global nutrition of the microalgal cell, which was most pronounced for exposure to 5 nm $nTiO_2$. The present study provides for the first-time evidence for the main metabolic perturbations in green alga *C. reinhardtii* exposed to $nTiO_2$ and helps to improve biological understanding of the molecular basis of these perturbations.

Received 18th March 2022,
Accepted 28th June 2022

DOI: 10.1039/d2en00260d

rsc.li/es-nano

Open Access Article. Published on 01 July 2022. Downloaded on 6/26/2024 11:57:25 PM.
This article is licensed under a Creative Commons Attribution 3.0 Unported Licence.

Environmental significance

A significant knowledge gap exists regarding the metabolic perturbations induced by engineered nanomaterials on phytoplankton species, in spite of their essential role in global biogeochemical cycles and food-web dynamics in aquatic environments. We have combined targeted metabolomics, transcriptomics and physiological response studies to explore quantitatively for the first time the metabolic alterations in green algae exposed to increasing concentrations of nano-sized titanium dioxide ($nTiO_2$) materials with three different primary sizes. We selected $nTiO_2$ as one of the most commonly used nanomaterials. Results revealed that exposure to $nTiO_2$ at concentrations higher than those usually found in freshwater environments induces significant alteration of the metabolism of amino acids, nucleotides, fatty acids, tricarboxylic acids and antioxidants, as well as disturbance of the global nutrient status of the algae. For most of the responsive metabolites the changes in the abundance upon $nTiO_2$ treatments were exposure concentration and primary size dependent.

Introduction

Nano-sized titanium dioxide ($nTiO_2$) is one of the top five most commonly used materials.[1,2] Recent measurements revealed that the concentrations of Ti-containing nanoparticles range between 10^4 and 10^7 nanoparticles per mL (corresponding to mass concentrations <10 μg L^{-1}) in global surface waters.[3] However in some hotspots, such as the runoff from the façade of a new building, much higher concentrations were detected.[4] Once released into the environment, $nTiO_2$ are subject of different physical, chemical and biological transformations, depending on the nanoparticle characteristics, environmental and biological factors.[5–7] $nTiO_2$ are considered as moderately stable in freshwater (global stability index of 0.46 for artificial freshwater).[8] Accompanying the well-established use and increasing environmental concentrations of $nTiO_2$, a significant amount of research has been conducted to assess their potential toxicity to different biota, including phytoplankton species.[9–16] $nTiO_2$ have been classified as "harmful" for the environment.[17] Evidence is accumulating that $nTiO_2$ can induce the enhanced production of reactive

[a] *University of Geneva, Faculty of Sciences, Earth and Environment Sciences, Department F.-A. Forel for Environmental and Aquatic Sciences, Environmental Biogeochemistry and Ecotoxicology, Uni Carl Vogt, 66 Blvd Carl-Vogt, CH 1211 Geneva, Switzerland. E-mail: vera.slaveykova@unige.ch*
[b] *Bren School of Environmental Science & Management, University of California, Santa Barbara, California 93106-5131, USA*

† Electronic supplementary information (ESI) available. See DOI: https://doi.org/10.1039/d2en00260d

This journal is © The Royal Society of Chemistry 2022

Open Access Article. Published on 01 July 2022. Downloaded on 6/26/2024 11:57:25 PM. This article is licensed under a Creative Commons Attribution 3.0 Unported Licence.

oxygen species (ROS) and oxidative stress,[7,9,18–21] the disruption of the cell membrane and interruption of energy transductions,[22] DNA and genotoxic damage[23,24] and the reduction of light available to algal cells due to the trapping of the algal cells in the $nTiO_2$ aggregates.[25] For a given organism, the toxicity of $nTiO_2$ depends on the size, crystalline structure and surface chemistry of nanoparticles in water.[26–29] The advances of 'omic' technologies allow a deeper insight into the metabolic perturbation in different phytoplankton species and the modes-of-action of environmental contaminants, including metal-containing nanoparticles.[30–35] For instance, $nCeO_2$ with different surface coatings affected the transcripts encoding flagella, indicating an effect on algal mobility.[36] Exposure to MoS_2 nanosheets altered significantly the nitrogen metabolism in cyanobacterium *Nostoc*.[37] Similarly, exposure of golden-brown alga *Poterioochromonas malhamensis* to nAg and released silver ions induced perturbation of the metabolism of amino acids, nucleotides, fatty acids, tricarboxylic acids, photosynthesis and photorespiration.[38] Dissolvable nAg decreased the abundance of D-galactose, sucrose, and D-fructose, carbohydrates involved in the synthesis and repair of cell walls, in a concentration dependent manner in *Scenedesmus obliquus*.[39] nAg affected the phosphorus assimilation metabolism in green alga *Chlorella vulgaris*[40] as well as altered the arginine and proline metabolism, indole alkaloid biosynthesis, and phospholipid metabolism in cyanobacterium *Microcystis aeruginosa*.[41] nAg exposure increased the levels of transcripts encoding components of the cell wall and the flagella *C. reinhardtii*.[42] Despite these advancements, little published research has focused on the cellular and molecular mechanisms involved in the stress tolerance of microalgae exposed to $nTiO_2$ with different primary sizes. The only "omic" study revealed that $nTiO_2$ raised the levels of transcripts encoding subunits of the proteasome, suggesting proteasome inhibition in *C. reinhardtii*.[42]

The main objective of the present study is to obtain a novel comprehensive understanding about the metabolic perturbations induced in microalgae exposed to $nTiO_2$. To this end, green alga *C. reinhardtii*, a representative aquatic primary producer, was exposed to increasing concentrations (2 to 200 mg L^{-1}) of $nTiO_2$ with primary sizes of 5, 15 and 20 nm for 72 h. We hypothesized that the observed metabolic perturbations will be dependent on the primary size and exposure concentration of $nTiO_2$. To verify this hypothesis, we have performed a targeted metabolomics study. The metabolomics results were further corroborated with the biological responses at physiological (growth inhibition, oxidative stress, membrane damage and changes in photosynthetic activity) and transcriptomic levels. In addition, the behaviour of $nTiO_2$ in the exposure medium was characterized in terms of aggregation and sedimentation. The findings of this exploratory study contribute to the improvement of the current knowledge regarding $nTiO_2$ toxicity pathways in this species, and possibly other species of microalgae.

Experimental

$nTiO_2$ materials

Powdered nano-sized TiO_2 particles with different primary sizes (anatase 5 nm (A5), anatase 15 nm (A15) and anatase/rutile 20 nm (AR20)) were purchased from Nanostructured & Amorphous Materials Inc, USA. The primary characteristics of the materials as provided by the manufacturer are given in Table S1, ESI.† Stock suspensions of 2.0 g L^{-1} $nTiO_2$ were prepared by dispersing nanoparticles in ultrapure water (Millipore, Darmstadt, Germany) using sonication for 10 min (50 W L^{-1} at 40 kHz). The stock suspensions were used to prepare suspensions of $nTiO_2$ in the exposure medium containing 2, 20, 100 and 200 mg L^{-1} of A5, A15 or AR20. The exposure medium consisted of 8.2×10^{-4} M $CaCl_2{\cdot}2H_2O$, 3.6×10^{-4} M $MgSO_4{\cdot}7H_2O$, 2.8×10^{-4} M $NaHCO_3$, 1.0×10^{-4} M KH_2PO_4 and 5.0×10^{-6} M NH_4NO_3 with a pH of 7.0 ± 0.2 and an ionic strength of 2.75 mM, as in our previous studies.[21,43] The selected test concentrations of $nTiO_2$ are much higher than those found in freshwater environments,[3] but cover a range of ecotoxicologically relevant concentrations.[44]

Characterization of $nTiO_2$ in algal exposure medium

The *Z*-average hydrodynamic diameter and zeta potential of the three types of $nTiO_2$ materials suspended in the exposure medium were measured at 72 h using a Malvern Zetasizer Nano-ZS (Malvern Instruments, Worcestershire, UK) at 20 °C. Results are the means of 3 sample measurements, 5 runs for each. The suspended fraction of the $nTiO_2$ suspensions was determined by using a UV-vis spectrophotometer (PerkinElmer UV/visible spectrophotometer Lambda 365, wave range of 200–800 nm) at the beginning of the experiment and at 72 h. The suspended fraction was determined as the ratio between the final (A) and initial absorbance (A_0) at the maximum absorption peak wavelength of 243 nm (A/A_0) as detailed previously.[43]

Bioassays with *Chlamydomonas reinhardtii*

Wild-type *C. reinhardtii* (CPCC11, Canadian Phycological Culture Centre, Waterloo, Canada) was grown axenically at 20.2 ± 0.5 °C, 115 rpm and 110 μmol phot m^{-2} s^{-1}. Algal cells were cultured in 4× diluted tris-acetate-phosphate (4× TAP) medium[45] until mid-exponential growth (62 hours post-inoculation), centrifuged (10 minutes, 1300*g*), rinsed and re-suspended (~10^6 cells per mL) in the exposure medium enriched with 2, 20, 100, and 200 mg L^{-1} A5, A15 or AR20 for 72 h. Negative controls (NC) in the absence of $nTiO_2$ were also performed. All the experiments were performed in 3 independent biological replicates. Changes in algal growth and physiology (excessive ROS generation, membrane damage and alteration of photosynthetic activity), alteration of key metabolites induced by $nTiO_2$ exposure and transcriptomic response were determined as presented below.

Open Access Article. Published on 01 July 2022. Downloaded on 6/26/2024 11:57:25 PM. This article is licensed under a Creative Commons Attribution 3.0 Unported Licence.

Evaluation of the $nTiO_2$ effect on algal growth and physiology

The effect of $nTiO_2$ on the algal growth was assessed following the changes of the algal cell densities by flow cytometry (FCM). The measurements were performed with a BD Accuri C6 flow cytometer equipped with a CSampler (BD Biosciences, San Jose, CA). The 488 nm argon excitation laser and fluorescence detection channels with band pass emission filters at 530 ± 15 nm (FL1), 585 ± 20 nm (FL2) and a long pass emission filter for >670 nm (FL3) were used. Data acquisition and analysis were performed with the BD Accuri C6 Software 264.15. The primary threshold was set to 20 000 events on FSC-H. Information on algal cell densities and chlorophyll fluorescence (in FL3) was obtained in a single run after 72 h incubation. Algal cells were discriminated from $nTiO_2$ aggregates with similar size by applying a gating strategy, as described in our earlier study.[21] The ROS generation and membrane damage were examined using the fluorescent probes CellROX® green (Life Technologies Europe B.V., Zug, Switzerland) and propidium iodide (PI) (Sigma-Aldrich, Buchs, Switzerland) and the number of affected cells was followed by FCM. The detailed staining procedures and gating strategies are presented in our previous studies.[21,46] The photosynthetic activity of *C. reinhardtii* was determined prior to and after $nTiO_2$ treatment using a Multiple Excitation Wavelength Chlorophyll Fluorescence Analyzer (Multi-Color-PAM, Walz, Germany). The maximal fluorescence yield of photosystem II, Fm, and maximal variable fluorescence, Fv (Fv/Fm) and non-photochemical quenching (NPQ) were measured after 72 h exposure following a 20 min dark acclimation. These parameters are well-known indicators for alteration of photosynthetic activity by different biotic and abiotic stressors.[38]

Assessment of the metabolic response by liquid chromatography-mass spectrometry targeted metabolomics

Changes in concentrations of key primary metabolites in *C. reinhardtii* exposed to the three $nTiO_2$ materials of different primary sizes at four concentrations (2, 20, 100, and 200 mg L^{-1}) and unexposed controls were determined by liquid chromatography-mass spectrometry (LC-MS) targeted metabolomics. At the end of the exposure for 72 h, the cells were placed in liquid nitrogen to stop metabolic activity, then frozen at −80 °C for 24 h and freeze-dried. Eighty metabolites, including antioxidants, amino acids, organic acids/phenolics, nucleobase/side/tide, sugar/sugar alcohols and fatty acids, were extracted in 80% methanol containing 2% formic acid, following a previously developed methodology.[38,47] Targeted analyses of these metabolites were performed using an Agilent 6470 liquid chromatography triple quadrupole mass spectrometer according to previously established methods.[47–50] The absolute concentrations of the metabolites in each sample were quantified using 7 point calibration standards, with isotopically-labeled metabolites as internal standards.

Statistical analyses of the metabolomics data were performed for exposed algae and control using MetaboAnalyst 5.0.[51] One-way analysis of variance (ANOVA) followed by Fisher's LSD *post hoc* analysis with $p < 0.05$ was completed to screen for metabolites differing between $nTiO_2$ treatments and controls, as well as differing between different $nTiO_2$ concentrations or primary sizes. Unsupervised principal component analysis (PCA) and supervised partial least squares-discriminant analysis (PLS-DA) were performed to get a global overview of the metabolic changes obtained in treatments with $nTiO_2$ of different primary sizes and different concentrations. Metabolites with a variable importance in the projection (VIP) greater than 1 were regarded as significant and responsible for group separation.[52] Metabolites significantly dysregulated by exposure to $nTiO_2$, as identified *via* ANOVA and PLS-DA, were further considered as responsive metabolites. Pathway analyses were performed with MetaboAnalyst 5.0 with respect to the KEGG pathway built-in metabolic library of green alga *Chlorella variables*.[53] Pathways with threshold >0.1 were considered as significantly dysregulated.[54,55]

Assessment of transcriptomic response using nCounter

To corroborate the results of targeted metabolomics, 117 transcripts were selected for analysis, including those involved in the response and toxicity pathway of *C. reinhardtii* to different pollutants[56] available in the Gene Expression Omnibus database (GSE65109). 94 of the transcripts have an annotation in MapMan ontology,[57] representing amino acid metabolism (16 transcripts), carbohydrate metabolism (17), stress (16), transport (30), metal binding (5) and photosynthesis (9). All selected transcripts were regulated by more than 2-fold in at least three conditions, and all of them had annotations to genes with known functions. Probes were designed and synthesized by NanoString nCounter Technologies (Table S2†). This technology offers a medium-throughput quantitative approach to study differential transcript expression. Total RNA was extracted from the *C. reinhardtii* exposed to the three types of $nTiO_2$ materials at two concentrations (2 and 20 mg L^{-1}) for 72 h. These concentrations were chosen based on the preliminary tests at exposure concentrations of 2, 20, 100 and 200 mg L^{-1} of $nTiO_2$ and considering the quality of extracted RNA. Untreated cells were used as control. For each replicate, approximately 100 mg fresh weight of algal cells from the control and experimental groups was harvested by centrifugation at 4 °C at 3200 × *g* for 5 min. Total RNA was extracted following the previously established protocol for *C. reinhardtii*.[58,59] The concentration of RNA was determined using the Qubit RNA Broad Range Assay Kit and a Qubit 2.0 fluorometer (Thermo Fisher Scientific, USA) following the manufacturer's instructions. The purity of RNA samples was estimated by assaying 2 μL of total RNA extract on a NanoDrop 2000c spectrophotometer (Thermo Scientific,

 This journal is © The Royal Society of Chemistry 2022

Open Access Article. Published on 01 July 2022. Downloaded on 6/26/2024 11:57:25 PM.
This article is licensed under a Creative Commons Attribution 3.0 Unported Licence.

USA). The quality of the RNA was confirmed (A 260/A 280: 1.8–2.0; A 260/A 230: 1.8–2.2).

100 ng of total RNA was hybridized with multiplexed Nanostring probes and samples were processed according to a published procedure.[60] Background correction was made by subtracting from the raw counts the mean ± 2 standard deviation of counts obtained with negative controls. Values <1 were fixed to 1 to avoid negative values after log transformation. Then, counts for target transcripts were normalized with the geometric mean of six housekeeping genes (Cre06_g260950_t1_2.1, Cre06_g272950_t1_1.1, Cre08_g370550_t1_1.1, Cre09_g411100_t1_2.1, Cre12_g519180_t1_1, Cre06_g260950_t1_2.1) selected as the most stable using the geNorm algorithm.[61] Normalized data were log 2 transformed for further analyses.

Statistical analysis of nCounter data was carried out with R, a free software environment available at **https://www.r-project.org**. After importing the normalized data, the significance of differential transcript expression between the groups was determined by computing the moderated *t*-statistics and false discovery rate (FDR) with the BioConductor package limma, available at **https://www.bioconductor.org**. *p*-Values were corrected for multiple testing by the use of the FDR method.[62] A significance threshold $p < 0.05$ associated with a fold change value of 2 or more was applied. Graphical representations were computed in GraphPad Prism 9.0 (Prism, GraphPad Software, San Diego).

Results and discussion

Characterization of $nTiO_2$ suspensions in the exposure medium

Since the stability of $nTiO_2$ dispersions in exposure medium plays an important role in the induced biological responses, we characterized $nTiO_2$ suspensions in the exposure medium in terms of their aggregation and sedimentation (Fig. 1). All three types of $nTiO_2$ aggregated substantially in the algal exposure medium at 72 h even at 2 mg L^{-1}, forming aggregates with sizes above 1000 nm (Fig. 1A). An increase of $nTiO_2$ concentration resulted in a rise in aggregate size, which was particularly pronounced for the A5 material with a primary size of 5 nm. The changes in average size with increasing concentration were less pronounced for A15 and AR20. A5 formed much bigger aggregates than A15 and AR20 at higher concentrations. For example, the *z*-average hydrodynamic diameter of A5 was about 3.9 times higher than those of A15 and AR20 in suspensions containing 200 mg L^{-1}. No significant difference was found between the aggregate size of A15 and AR20 at the four tested concentrations. All $nTiO_2$ suspensions in exposure medium exhibited a negative zeta potential value (Fig. 1B): −18.1 mV for A5, −15.3 mV for A15 and −13.4 mV for AR20 at a concentration of 2 mg L^{-1}. Increasing $nTiO_2$ concentration resulted in a significant decrease in the absolute values of the zeta potential for the three tested $nTiO_2$ materials, which was consistent with the formation of bigger $nTiO_2$ aggregates. As shown in our preceding studies, the three $nTiO_2$ materials form rapidly micrometer aggregates in the exposure medium (2 h exposure,[21]) and the size of the aggregates stayed stable over the time interval 24–96 h.[43]

The percentage of suspended TiO_2 decreased with increasing concentration (Fig. 1C), reflecting the larger aggregates formed at higher concentrations and their sedimentation rates. For example, only about 19%, 32% and 88% of particles for A5, A15 and AR20, respectively, were still suspended after 72 h at a concentration of 2 mg L^{-1}. Our previous kinetic study revealed that the micrometer aggregates of $nTiO_2$ settled down rapidly within the first 24 h and the percentage of the suspended particles tended to stay constant from 24 to 96 h.[43] The above observations are consistent with the fact that the $nTiO_2$ suspensions at higher concentrations are more susceptible to aggregation due to the increased collision probability between the particles.[63] It is currently accepted that the aggregation state of $nTiO_2$ suspensions is a result of the van der Waals attraction forces,[64] Coulomb repulsion caused by the surface charge of the particles or the action of the electrostatic double layer, and steric hindrance.[65]

Effect of $nTiO_2$ treatments on algal physiology

All three tested $nTiO_2$ materials induced growth inhibition in less than 50% of the exposed alga and the effect was

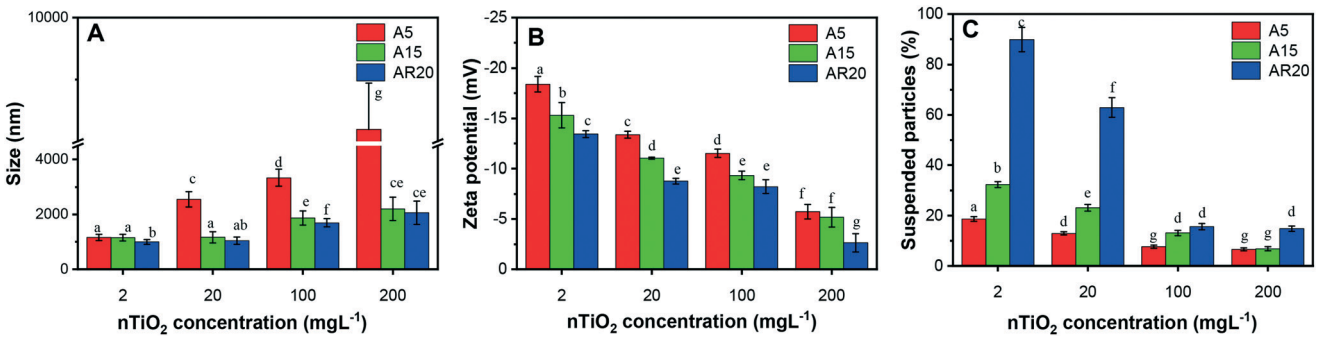

Fig. 1 Characterization of the stability at 72 h in the exposure medium of $nTiO_2$ at concentrations of 2, 20, 100 and 200 mg L^{-1}. (A) TiO_2 *z*-average hydrodynamic diameter; (B) TiO_2 zeta potential; (C) sedimentation of $nTiO_2$. Different letters indicate statistically significant differences between the values as obtained by ANOVA and a Tukey's *post hoc* test ($p < 0.05$).

Open Access Article. Published on 01 July 2022. Downloaded on 6/26/2024 11:57:25 PM.
This article is licensed under a Creative Commons Attribution 3.0 Unported Licence.

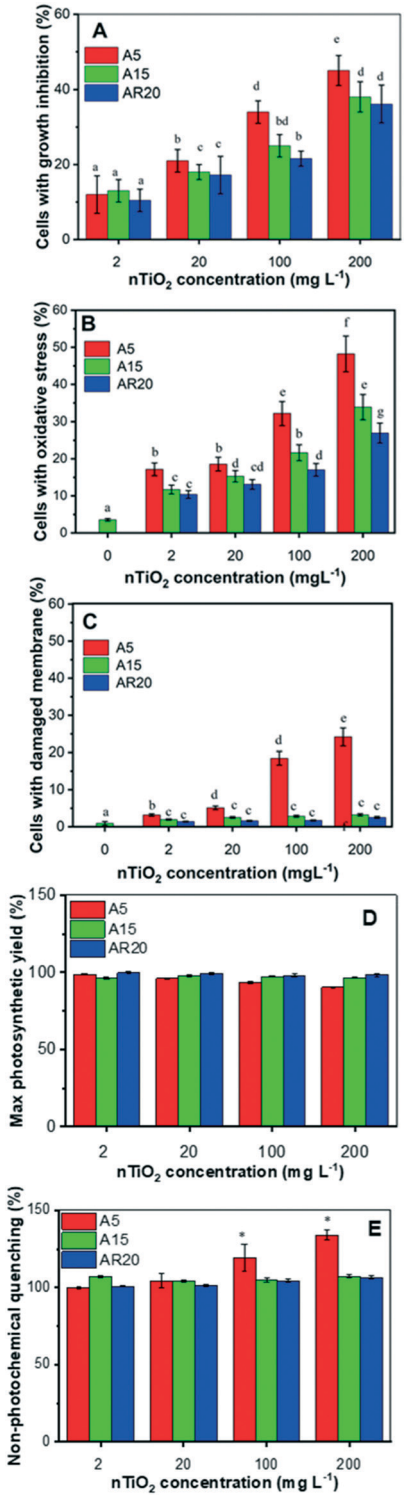

Fig. 2 Effect of $nTiO_2$ on (A) the percentage of cells with inhibited growth, (B) the percentage of cells with oxidative stress, (C) the percentage of cells with membrane damage, (D) cells with the maximum quantum yield of photosystem II (Fv/Fm) as a % of control, and (E) non-photochemical quenching (NPQ) as a % of control in *C. reinhardtii* exposed to three different materials: A5, A15 and AR20. (A and B) Different letters indicate statistically significant differences between the values as obtained by ANOVA and a Tukey's *post hoc* test ($p < 0.05$). (C and D) * indicate statistically significant differences between the values as obtained by ANOVA and a Tukey's *post hoc* test ($p < 0.05$).

concentration dependent (Fig. 2A). Exposure to A5 resulted in the most important growth inhibition, compared with the A15 and AR20 treatments, showing that the $nTiO_2$ with lower size inhibited the growth of *C. reinhardtii* more significantly ($p < 0.05$). These observations agree with the finding that the toxicity outcome of exposure to $nTiO_2$ depends on the primary size.[20,27,29] These findings would also suggest that *C. reinhardtii* is more tolerant to $nTiO_2$ in comparison with other green algae and diatoms.[20,28,29,44] However, direct comparison is not possible given different exposure medium compositions and different $nTiO_2$ materials used. The generation of excessive cellular ROS concentrations is considered the most likely toxicity mechanism of $nTiO_2$.[20] Here all three types of $nTiO_2$ induced oxidative stress in *C. reinhardtii* even at the lowest tested concentration of 2 mg L^{-1} (Fig. 2B). The oxidative stress became more pronounced with increasing $nTiO_2$ concentration for all tested materials. A5 induced stronger oxidative stress than A15 and AR20, as already observed at short term exposure.[21]

Changes in membrane permeability induced by 72 h-exposure to A15 and AR20 were negligible. The percentage of affected cells was comparable to unexposed controls. However, exposure of *C. reinhardtii* to A5 resulted in a significant percentage of cells with membrane damage at a $nTiO_2$ concentration of 200 mg L^{-1} (Fig. 2C). This result is also consistent with the observed trapping of the algal cells in aggregates of A5 at 96 h exposure.[43]

$nTiO_2$ treatments had no measurable effect on algal photosynthesis. No significant difference ($p > 0.05$) of the Fv/Fm and NPQ values was found in all treatments except for A5 at a concentration of 200 mg L^{-1} in comparison with the control after 72 h (Fig. 2D and E). The decrease in Fv/Fm reveals an inhibition in algal photosynthetic activity related to light energy utilization caused by 200 mg L^{-1} A5. In agreement with Fv/Fm, no significant differences in NPQ were observed after exposure to the three $nTiO_2$ materials. A significant effect ($p < 0.05$) on NPQ was found only upon exposure to 200 mg L^{-1} A5, indicating that the absorbed light energy exceeded the capacity of its utilization in photosynthetic processes, considered as a primary defense mechanism employed to dissipate the stress.

Overview of metabolic profiles in *C. reinhardtii* under different $nTiO_2$ treatments

Of a total of 80 metabolites analyzed, 50 were found above their limits of detection and determined in the controls and treatments with $nTiO_2$ of different primary sizes and concentrations. A general overview of the different treatment groups was obtained by unsupervised PCA (Fig. S1†) and supervised PLS-DA for concentration treatments (Fig. 3) and different size treatments (Fig. S2† and 4). The PLS-DA score plot (Fig. 3A and B) showed excellent separation of A5 and A15 treatments and unexposed controls, as well as treatments with different $nTiO_2$ concentrations, highlighting the importance of tracking the alteration of the metabolic

 This journal is © The Royal Society of Chemistry 2022

Open Access Article. Published on 01 July 2022. Downloaded on 6/26/2024 11:57:25 PM.
This article is licensed under a Creative Commons Attribution 3.0 Unported Licence.

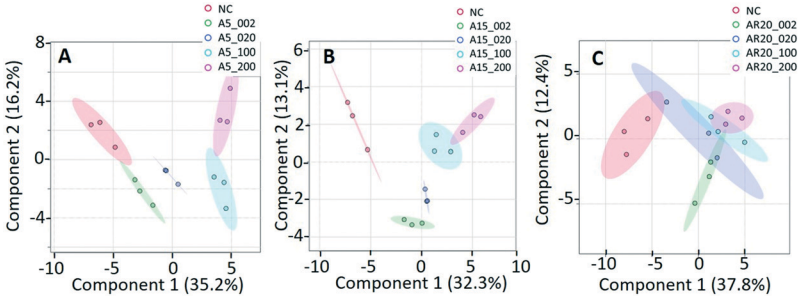

Fig. 3 Analysis of metabolic response of *C. reinhardtii* treated with increasing concentrations of three $nTiO_2$ materials by partial least-squares discriminate analysis (PLS-DA) score plots: treatments with: (A) 5 nm $nTiO_2$ 2 mg L^{-1} (A5_2), 20 mg L^{-1} (A5_20), 100 mg L^{-1} (A5_100) and 200 mg L^{-1} (A5_200); (B) 15 nm $nTiO_2$ 2 mg L^{-1} (A15_2), 20 mg L^{-1} (A15_20), 100 mg L^{-1} (A15_100) and 200 mg L^{-1} (A15_200); (C) 20 nm $nTiO_2$ (AR20): 2 mg L^{-1} (AR20_2), 20 mg L^{-1} (AR20_20), 100 mg L^{-1} (AR20_100) and 200 mg L^{-1} (AR20_200); negative control (NC). Data were row-wise normalized using probabilistic quotient normalization by reference groups, non-transformed and autoscaled. The score plots and heatmap were generated using MetaboAnalyst 5.0 (**https://www.metaboanalyst.ca/**).

response with exposure concentrations. For the AR20 exposure, the separation of the $nTiO_2$ treatments from controls and among the treatments was not very good (Fig. 3C). Based on a VIP score >1 (Fig. S3†) and ANOVA (Tables S3–S5†), a total of 26 responsive metabolites were identified to be significant in the A5-treatments in comparison with the untreated control; 25 for A15 and 26 for AR20.

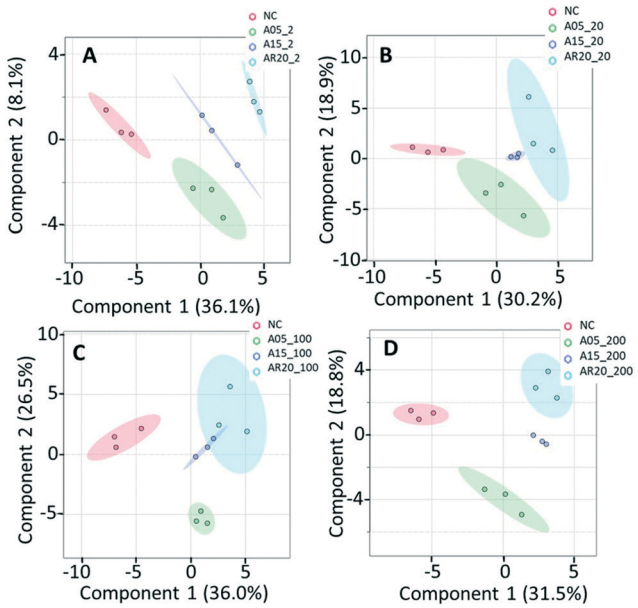

Fig. 4 PLS-DA of metabolic response of *C. reinhardtii* treated with $nTiO_2$ materials of different primary sizes. Treatments with: (A) 2 mg L^{-1} of $nTiO_2$ with a size of 5 nm (A5_002), 15 nm (A15_002) and 20 nm (AR20_002); (B) 20 mg L^{-1} of $nTiO_2$ with a size of 5 nm (A5_020), 15 nm (A15_020) and 20 nm (AR20_020); (C) 100 mg L^{-1} of $nTiO_2$ with a size of 5 nm (A5_100), 15 nm (A15_100) and 20 nm (AR20_100); (D) 200 mg L^{-1} of $nTiO_2$ with a size of 5 nm (A5_200), 15 nm (A15_200) and 20 nm (AR20_200); negative control (NC). Data were row-wise normalized using probabilistic quotient normalization by reference groups, non-transformed and autoscaled. The score plots are generated by MetaboAnalyst 5.0 (**https://www.metaboanalyst.ca/**).

The results of the supervised PLS-DA for treatments with a given concentration of $nTiO_2$ of different primary sizes (Fig. 4) showed very good separation between the control and different primary size treatments for all concentrations, demonstrating the importance of considering the primary size of $nTiO_2$ in metabolic perturbations. Based on a VIP score >1 (Fig. S4†) and ANOVA (Tables S6–S9†), a total of 28 responsive metabolites were found for 2 mg L^{-1}, 21 for 20 mg L^{-1}, 34 for 100 mg L^{-1} and 29 for 200 mg L^{-1} $nTiO_2$, for different size treatments. With a small exception, the abundance of the same metabolites was affected in different treatments with a rather clear size dependence for the same initial $nTiO_2$ concentration. It is necessary to keep in mind that in addition to the differences in size there is a small difference in the crystalline structure: A5 and A15 are composed of anatase, whereas AR20 contains 80–90% anatase and 10–20% rutile. $nTiO_2$ in anatase crystal structure was shown to be more toxic for algae than rutile.[28]

Overall, most of the responsive metabolites were common for different $nTiO_2$ concentration- and size-treatments. They included mainly amino acids, antioxidants, some fatty and carboxylic acids and nucleobases/sides/tides. However, the intensity of the responses and size- or concentration-dependences differed, as discussed further.

The responsive metabolites were also grouped by heatmap clustering. In different concentration treatments (Fig. S5–S7†), three large groups were identified corresponding to (i) metabolites with *higher abundance* in algae treated with $nTiO_2$ than in the control (12 for A5, 12 for A15 and 15 for AR20). In the group, the metabolites with increasing abundance with the $nTiO_2$ concentrations were 9 for A5, 5 for A15, and 5 for AR20; (ii) metabolites with *lower abundance* in $nTiO_2$ treatments than in the untreated control (11 for A5, 11 for A15 and 12 for AR20). Within this group, the number of metabolites with decreasing abundance with $nTiO_2$ concentrations was 9 for A5, 11 for A15, and 10 for AR20; and (iii) metabolites with no clear concentration dependence.

Open Access Article. Published on 01 July 2022. Downloaded on 6/26/2024 11:57:25 PM.
This article is licensed under a Creative Commons Attribution 3.0 Unported Licence.

Clustering of the treatments as a function of the primary size of $nTiO_2$ revealed five clusters including (Fig. S8–S11†): (i) metabolites with *higher abundance* than the control; increase of metabolite concentrations with primary size (metabolites with the *highest abundance* in AR20 treatments: 11 at 2 mg L^{-1}, 8 at 20 mg L^{-1}, 3 at 100 mg L^{-1}, 1 at 200 mg L^{-1}); (ii) metabolites with *higher abundance* than the control, decrease of metabolite concentrations with primary size (metabolites with the *highest abundance* in A5 treatments: 2 at 2 mg L^{-1}, 2 at 20 mg L^{-1}, 11 at 100 mg L^{-1}, 8 at 200 mg L^{-1}); (iii) metabolites with *lower abundance* than the control; decrease of the metabolite concentrations with the primary size (metabolites with the *lowest abundance* in AR20 treatments: 7 at 2 mg L^{-1}, 7 at 20 mg L^{-1}, 7 at 100 mg L^{-1}, 6 at 200 mg L^{-1}); (iv) metabolites with *lower abundance* than the control; increase of the metabolite concentration with primary size (metabolites with the lowest abundance in A5 treatments – 6 at 2 mg L^{-1}, 3 at 20 mg L^{-1}, 6 at 100 mg L^{-1}, 5 at 200 mg L^{-1}). The number of metabolites with the highest or lowest abundance at 2 and 20 mg L^{-1} for AR20 treatments could be related to the much higher percentage of AR20 dispersed in the suspensions of 2 and 20 mg L^{-1} $nTiO_2$ than 100 and 200 mg L^{-1} $nTiO_2$ treatments; (v) metabolites with no clear concentration dependence.

Furthermore, the responsive metabolites identified by PLS-DA and ANOVA corresponded to 11impacted pathways (Fig. S12 and S13†). Interestingly, the number of the significantly impacted pathways increased with the decrease of the primary size (Fig. S12†) and the increase of $nTiO_2$ exposure concentrations (Fig. S13†). The glutathione metabolism, alanine, aspartate and glutamate metabolism, cysteine and methionine metabolism, phenylalanine metabolism and arginine biosynthesis were commonly affected in different treatments. Exposure to A5 resulted in the strongest impact on the glutathione metabolism.

Overview of transcriptomic profiles in *C. reinhardtii* under different $nTiO_2$ treatments

PCA and PLS-DA of the differences in transcript expression between the unexposed controls, treatments with $nTiO_2$ of different concentrations (Fig. S14† and 5) and different primary sizes (Fig. S15† and 6) were conducted. A good separation of A5 and AR20 treatments from the control as well as treatments with different concentrations of $nTiO_2$ was observed (Fig. 5A and C). Poor separation between A15 treatments and the control was found (Fig. 5B).

At 2 mg L^{-1} no separation between the treatments with different sizes and controls was observed (Fig. 6A). However, at 20 mg L^{-1}, good separation of the treatments with all three $nTiO_2$ materials and controls was found. In addition, the distribution of principal components of A5 was clearly separate from A15 and AR20 (Fig. 6B). These results highlighted that the three $nTiO_2$ altered significantly the transcriptomic expression in *C. reinhardtii* in a primary size dependent way at concentrations of 20 mg L^{-1}.

Of the 117 transcripts tested with nCounter, only a few transcripts allowed discrimination between the treatments. For A5 treatment, the abundance of 3 and 49 transcripts was significantly altered upon exposure to A5 at 2 (Fig. S16A†) and 20 mg L^{-1} (Fig. S16B†), respectively. However, the expression of few transcripts was significantly altered in A15 and AR20 treatments: 9 for A15 at 2 and 20 mg L^{-1} (Fig. S16C and D†), 3 and 8 for AR20 at 2 and 20 mg L^{-1} (Fig. S16E and F†), respectively. This analysis confirmed that for exposure to 20 mg L^{-1}, $nTiO_2$ of smaller primary size (A5) has a significantly larger effect on transcriptome expression of *C. reinhardtii* when compared with the A15 and AR20 treatments. The number of upregulated transcripts for both treatments was larger than the downregulated transcripts. Despite the observed increase in the number of transcripts with dysregulated expression observed for A5, it is not

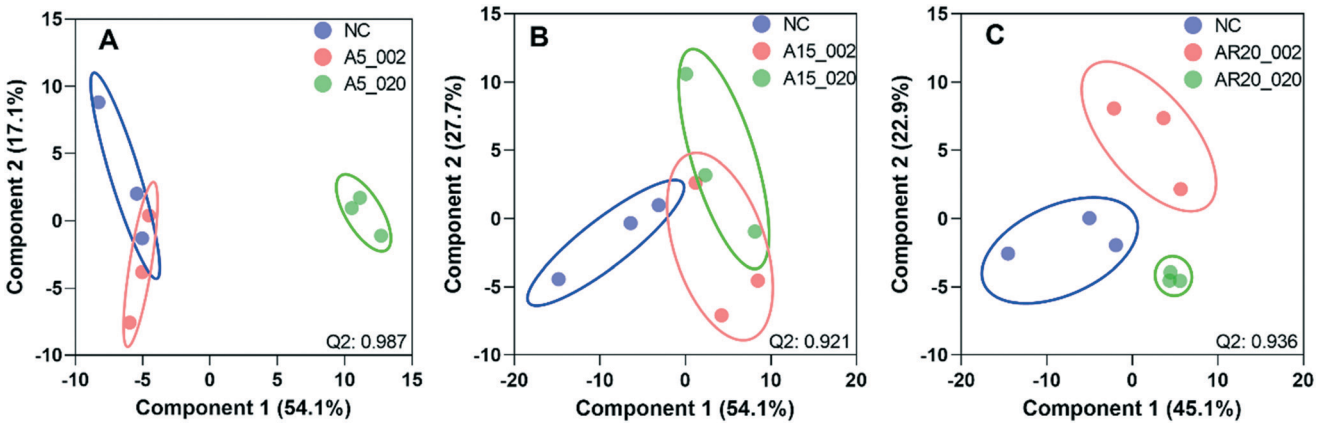

Fig. 5 PLS-DA of transcript expression of *C. reinhardtii* exposed to 2 and 20 mg L^{-1} of three types of $nTiO_2$. (A) Treatments with A5 at 2 mg L^{-1} (A5_002) and 20 mg L^{-1} (A5_020). (B) Treatments with A15 at 2 mg L^{-1} (A5_002) and 20 mg L^{-1} (A5_020). (C) Treatments with AR20 at 2 mg L^{-1} (A5_002) and 20 mg L^{-1} (A5_020); negative control (NC). The significance of differential transcript expression between the groups was determined by computing the moderated *t*-statistics and FDR with the BioConductor package limma in R. Q2 values for cross validation of the models are also given.

 This journal is © The Royal Society of Chemistry 2022

Open Access Article. Published on 01 July 2022. Downloaded on 6/26/2024 11:57:25 PM.
This article is licensed under a Creative Commons Attribution 3.0 Unported Licence.

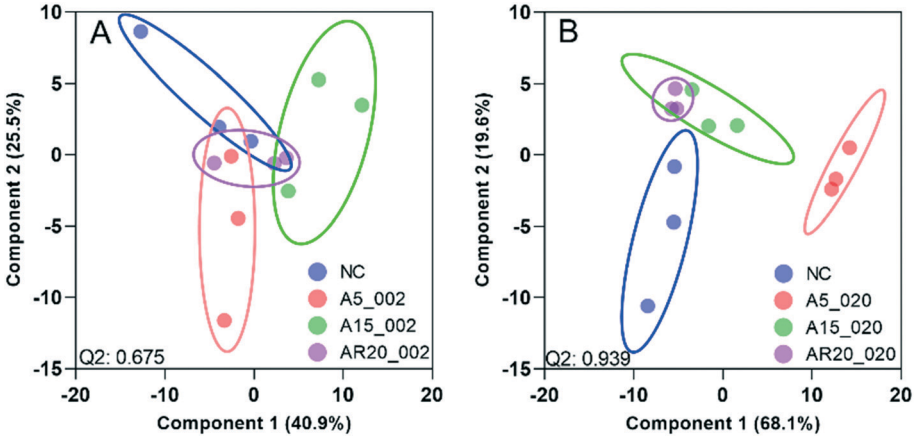

Fig. 6 PLS-DA of transcript expression of *C. reinhardtii* exposed to $nTiO_2$ of 5, 15 and 20 nm primary size at 2 and 20 mg L^{-1}. (A) Treatments with A5 at 2 mg L^{-1} of A5 (A5_002), A15 (A 15_002) and AR20 (AR20_002). (B) Treatments with A5 at 20 mg L^{-1} of A5 (A5_020), A15 (A 15_020) and AR20 (AR20_020); negative control (NC). The significance of differential transcript expression between the groups was determined by computing the moderated *t*-statistics and FDR with the BioConductor package limma in R. Q2 values for cross validation of the models are also given.

possible to make conclusions about the concentration dependence of the responses, given the impossibility to extract RNA of good quality in the treatments with 100 and 200 mg L^{-1} $nTiO_2$. Moreover, 36.7% of dysregulated genes had a fold change >4 or <−4 in 20 mg L^{-1} A5 treatment, suggesting that the exposure to the smaller size at the higher concentration of 20 mg L^{-1} $nTiO_2$ resulted in a stronger dysregulation than other treatments.

Significantly dysregulated transcripts corresponded to biological pathways that include regulation of cell processes, energy metabolism (photosynthesis, carbohydrate metabolism), amino acid metabolism, stress and transport

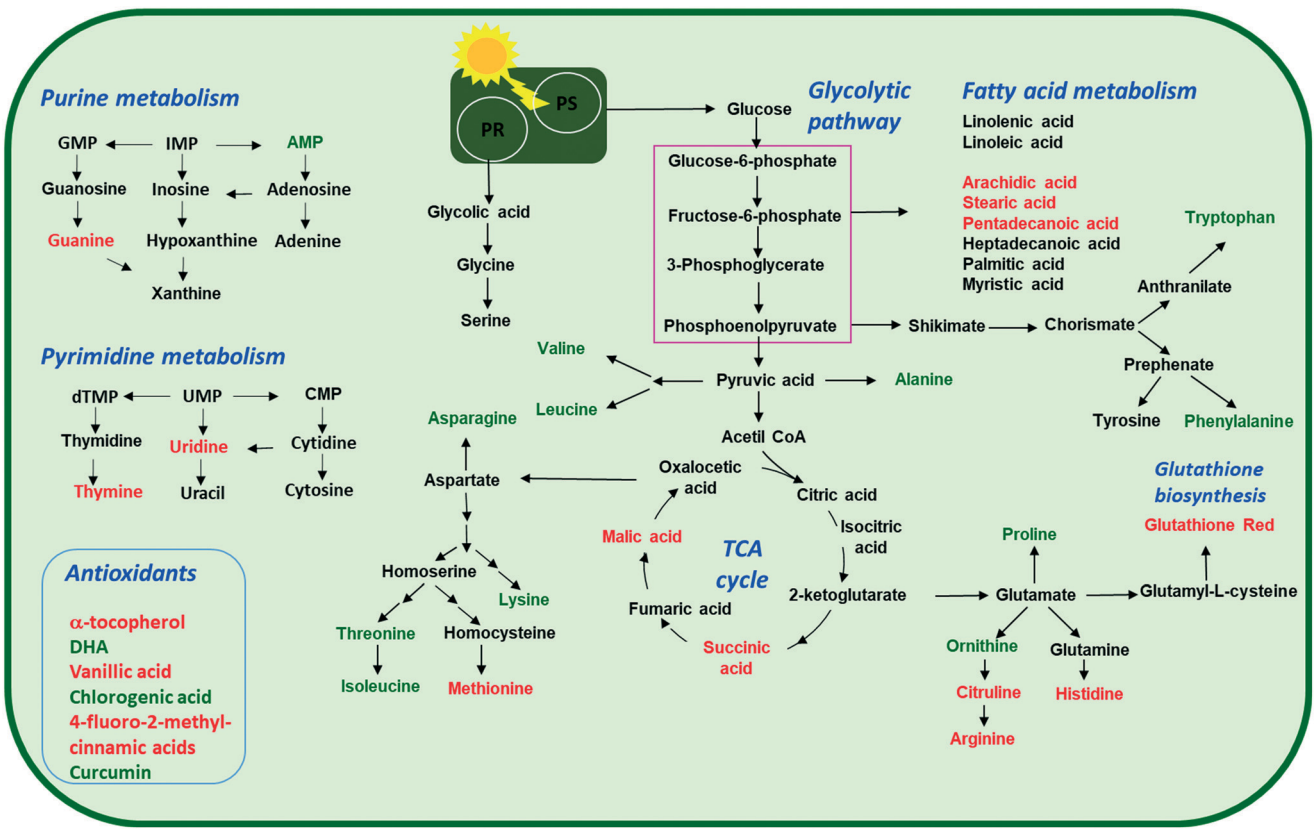

Fig. 7 Overview of the proposed perturbations in metabolic pathways in green alga *C. reinhardtii* alga exposed to increasing concentrations (2, 20, 100 and 200 mg L^{-1}) of $nTiO_2$ with primary size of 5, 15 and 20 nm for 72 h. Accumulated or depleted responsive metabolites are present in red and green colors, respectively. PS: photosynthesis; PR: photorespiration. Only responsive metabolites were considered.

Open Access Article. Published on 01 July 2022. Downloaded on 6/26/2024 11:57:25 PM.
This article is licensed under a Creative Commons Attribution 3.0 Unported Licence.

(Fig. S17, Table S10†), thus providing an indication about the cellular targets in *C. reinhardtii.* The number of dysregulated genes depended on the primary size of the tested $nTiO_2$ and increased with concentration from 2 to 20 mg L^{-1}. The exposure to two lower concentrations of $nTiO_2$ resulted in significant changes in the adaptation of the nutrition pathways and metabolic production of energy as well as the induction of oxidative stress, and consequently, the activation of cellular protective response.

Metabolic perturbation in *Chlamydomonas reinhardtii* exposed to $nTiO_2$

Amino acid metabolism. Exposure to different $nTiO_2$ induced a significant alteration in the abundance of 15 amino acids out of 21 amino acids that were quantified in *C. reinhardtii* (Fig. 7). *Alanine*, *leucine* and *valine* (Fig. 8A) produced from pyruvate[66] were significantly reduced ($p < 0.05$) in A5 exposed cells. The reduction of these three metabolites was most important for the smallest size of the tested $nTiO_2$ (A5) with a stronger decrease at higher exposure concentrations. *Leucine* concentrations were reduced in the treatments with A5 and A15, however no dependence on the exposure concentrations was observed for AR20. *Leucine*, a branched chain amino acid, serves as an oxidative phosphorylation energy source or as a detoxification pathway;[67] its depletion may indicate that it was employed as a defense. Concentration dependent depletion of *valine* was induced only in A5, but not in A15 and AR20 exposures. The abundance of the amino acids derived from aspartate *asparagine*, *lysine* and *threonine* (Fig. 8) was significantly decreased with respect to the control with clear size and

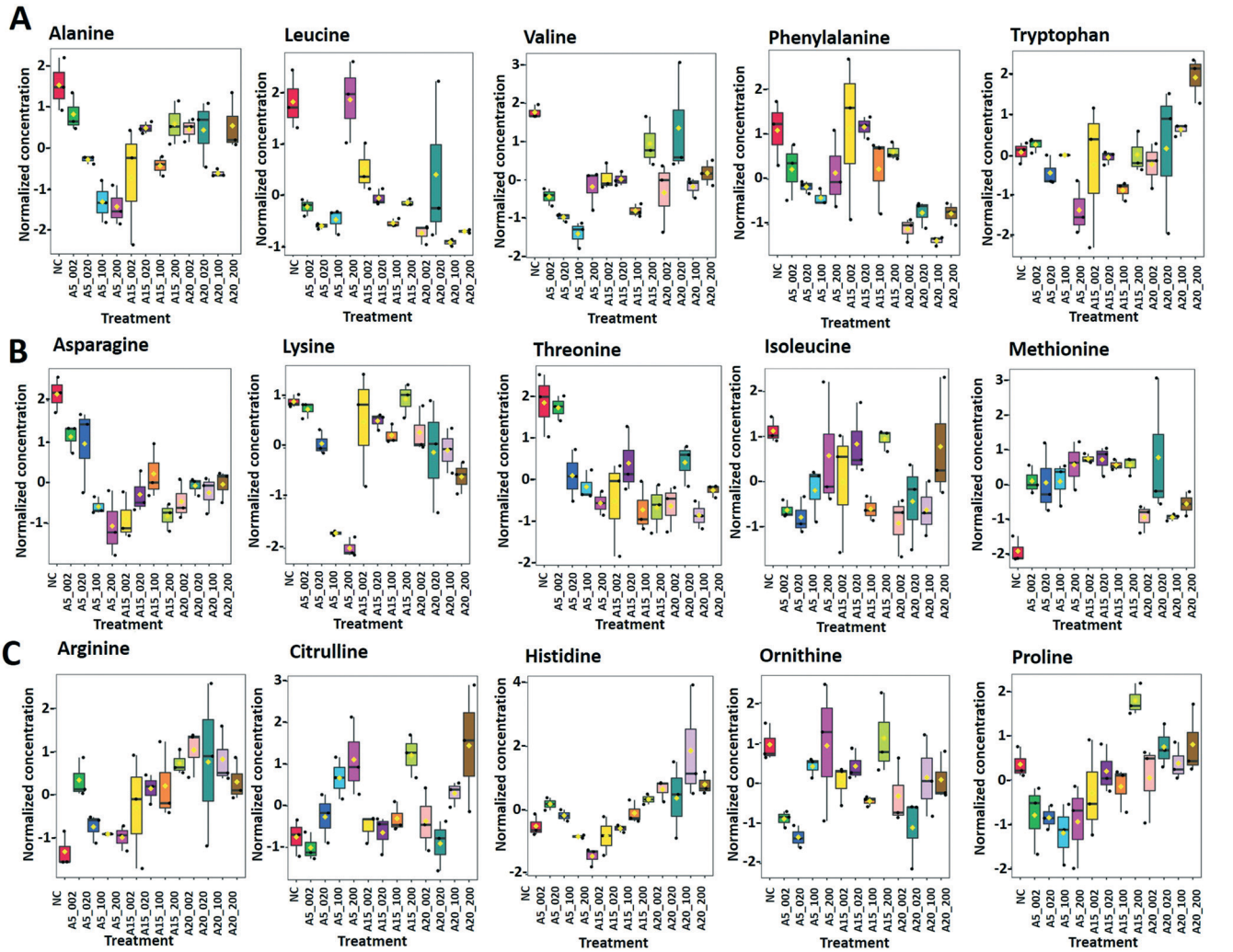

Fig. 8 Box plots of relative abundance of (A) amino acids alanine, leucine, valine, phenylalanine and tryptophan, (B) aspartate-derived amino acids, and (C) α-ketoglutarate-derived amino acids responsive to treatment of *C. reinhardtii* with 2–200 mg L^{-1} $nTiO_2$ with primary size of 5, 15 and 20 nm: treatments with: 5 nm $nTiO_2$ 2 mg L^{-1} (A5_2), 20 mg L^{-1} (A5_20), 100 mg L^{-1} (A5_100) and 200 mg L^{-1} (A5_200); 15 nm $nTiO_2$ 2 mg L^{-1} (A15_2), 20 mg L^{-1} (A15_20), 100 mg L^{-1} (A15_100) and 200 mg L^{-1} (A15_200); 20 nm $nTiO_2$ (AR20): 2 mg L^{-1} (AR20_2), 20 mg L^{-1} (AR20_20), 100 mg L^{-1} (AR20_100) and 200 mg L^{-1} (AR20_200); negative control (NC). Data were row-wise normalized using probabilistic quotient normalization by reference groups, non-transformed and autoscaled.

 This journal is © The Royal Society of Chemistry 2022

Open Access Article. Published on 01 July 2022. Downloaded on 6/26/2024 11:57:25 PM. This article is licensed under a Creative Commons Attribution 3.0 Unported Licence.

concentration dependences at A5 treatments. As *asparagine* is involved in ammonium assimilation in plants,[68] it could be hypothesized that the capacity to acquire nitrogen compounds is partially inhibited by the $nTiO_2$ treatments. The abundance of *isoleucine* was lower in $nTiO_2$ cells than in the control, however the decrease was more substantial for treatments at lower $nTiO_2$ concentration. *Methionine* accumulated in treatments with the three $nTiO_2$ materials in comparison with the controls. The abundance of *methionine* significantly increased with increasing concentrations of A5, however a less clear concentration dependence was found in A15 and AR20 exposures. A clear dependence on the primary size of $nTiO_2$ was observed in 100 and 200 mg L^{-1} treatments, with A5 being the most responsive. *Methionine* is the first amino acid to be translated in protein synthesis by initiating mRNA translation and is the precursor of essential biomolecules through *S*-adenosylmethionine.[69] Changes in its abundance could be used to provide an estimate of the rate of protein synthesis.[70] Therefore, the accumulation of this metabolite suggests a significant acceleration of the rate of protein synthesis in A5 treatments.

Arginine, *citrulline* and *histidine* (Fig. 8C) biosynthesized from the TCA metabolite α-ketoglutarate[71] increased in cells exposed to the three $nTiO_2$. The abundance of *citrulline* increased with higher $nTiO_2$ exposure concentrations, as well as the abundance of *arginine* in A15 and AR20 treatments.

Ornithine was depleted in $nTiO_2$ treatments with respect to the control and the depletion was more pronounced for A5. *Histidine* and *proline* exhibited a more complex pattern with an increase in abundance with exposure concentration for A15, a decrease for A5 and lack of concentration dependence for AR20 treatments. As it is an amino acid needed for growth and development of algal cells,[72] the accumulation reveals an impact on algal growth and cell development. In addition, *histidine* and *arginine* take part in deamination,[73] showing that this process can be also altered. *Proline* plays an important role in osmo- and redox-regulation, metal chelation, and scavenging of free radicals induced by different metals in plants,[74,75] therefore a decrease in abundance suggests a defensive response to oxidative stress.

Levels of aromatic amino acids, *phenylalanine* and *tryptophan*, derived from phosphoenolpyruvate were significantly reduced in a concentration dependent manner in A5 treatments only. Concentrations of two other amino acids, *glycine* and *serine*, measured in $nTiO_2$ treatments and controls were comparable. As these amino acids are synthesized by the photorespiratory glycolate cycle in algae,[66] the fact that no changes were observed in their concentration suggests no effect of $nTiO_2$ on algal photorespiratory activity. These findings are in line with no observed changes in maximum photosynthetic yield and NPQ in most $nTiO_2$ treatments (Fig. 2D and E), as well as with the lack of changes in the abundance of glucose which is a primary product of photosynthesis.

The metabolomics results are consistent with the strong dysregulation of the following transcripts involved in amino-acid metabolism. Four transcripts involved in amino acid metabolism were significantly affected by exposure to A5 at 20 mg L^{-1}, but not to A15 and AR20 (Table S10†). The transcripts in genes coding for "phosphoserine aminotransferase" involved in the phosphorylated pathway of serine biosynthesis[76] (Cre07.g331550.t1.2, FC −2.81, FDR 7.63×10^{-9}) and "dihydrodipicolinate reductase" involved in L-lysine biosynthesis[77] (Cre16.g656300.t1.3, FC −2.07, FDR 6.77×10^{-7}), as well as peroxisomal 3-ketoacyl-CoA thiolase 3 in the isoleucine degradation pathway[78] (Cre17.g723650.t1.2, FC −2.08, FDR 7.63×10^{-9}), were down-regulated. The transcripts coding for fumarylacetoacetate hydrolase, which are involved in the final step of the tyrosine degradation pathway[79] (Cre12.g549450.t1.2, FC 4.50, FDR 3.45×10^{-10}), were up-regulated.

Nucleobase/tide/side metabolism. Among 15 nucleobases/tides/sides considered, 6 were quantified and 4 were statistically different from control treatments ($p < 0.05$) (Fig. 7 and 9A). The *pyrimidine* nucleotides/sides *uridine* and *thymine* accumulated in $nTiO_2$ treatments. The *thymine* concentration increased with A5, A15 and AR20 concentrations. The *purine* metabolites (*AMP*, *guanine)* significantly increased in algae exposed to $nTiO_2$ as compared with unexposed controls. *Guanine* levels rise with the exposure concentrations of A5 and A15; however, no concentration- or size-dependences were observed for AR20 treatments. A decrease of the abundance of AMP with the concentration of the $nTiO_2$ was observed. Pyrimidine and purine nucleotides are structural elements of the nucleic acids DNA and RNA.[80] Therefore, the present results could suggest an acceleration of DNA and RNA synthesis and turnover.

Antioxidant metabolism. Exposure to the $nTiO_2$ with a primary size of 5 nm resulted in a significant increase of the abundance of *reduced glutathione* (GSH) in comparison with the control (Fig. 9B). Interestingly the increase was pronounced at lower concentrations of $nTiO_2$ and decreased with an increase of the exposure concentration. This result suggests an activation of the defense mechanism against the oxidative stress induced by $nTiO_2$, since GSH is central to redox control in the cell.[81] Nevertheless, a significant generation of the ROS was found in *C. reinhardtii* exposed to $nTiO_2$ (Fig. 2B). The above observation is consistent with the existing literature for metals and metal-containing NPs showing an increased level of GSH in green algae exposed to high concentrations of Cd^{2+} (ref. 82 and 83) or inorganic or monomethyl MeHg,[47] whereas Cu exposure decreased GSH concentrations.[83,84] Exposure of *P. melhamensis* to nAg and Ag ions also resulted in an accumulation of reduced GSH, which increased with the exposure time from 2 to 24 h.[38]

Dehydroascorbic acid (DHA, Fig. 9B), an oxidized form of ascorbic acid, was significantly depleted in the treatments with all three $nTiO_2$ as compared with the control. However, no clear dependence on the concentration as a function of $nTiO_2$ primary size or exposure concentration was found. Such a decrease of DHA probably corresponds to its

Open Access Article. Published on 01 July 2022. Downloaded on 6/26/2024 11:57:25 PM.
This article is licensed under a Creative Commons Attribution 3.0 Unported Licence.

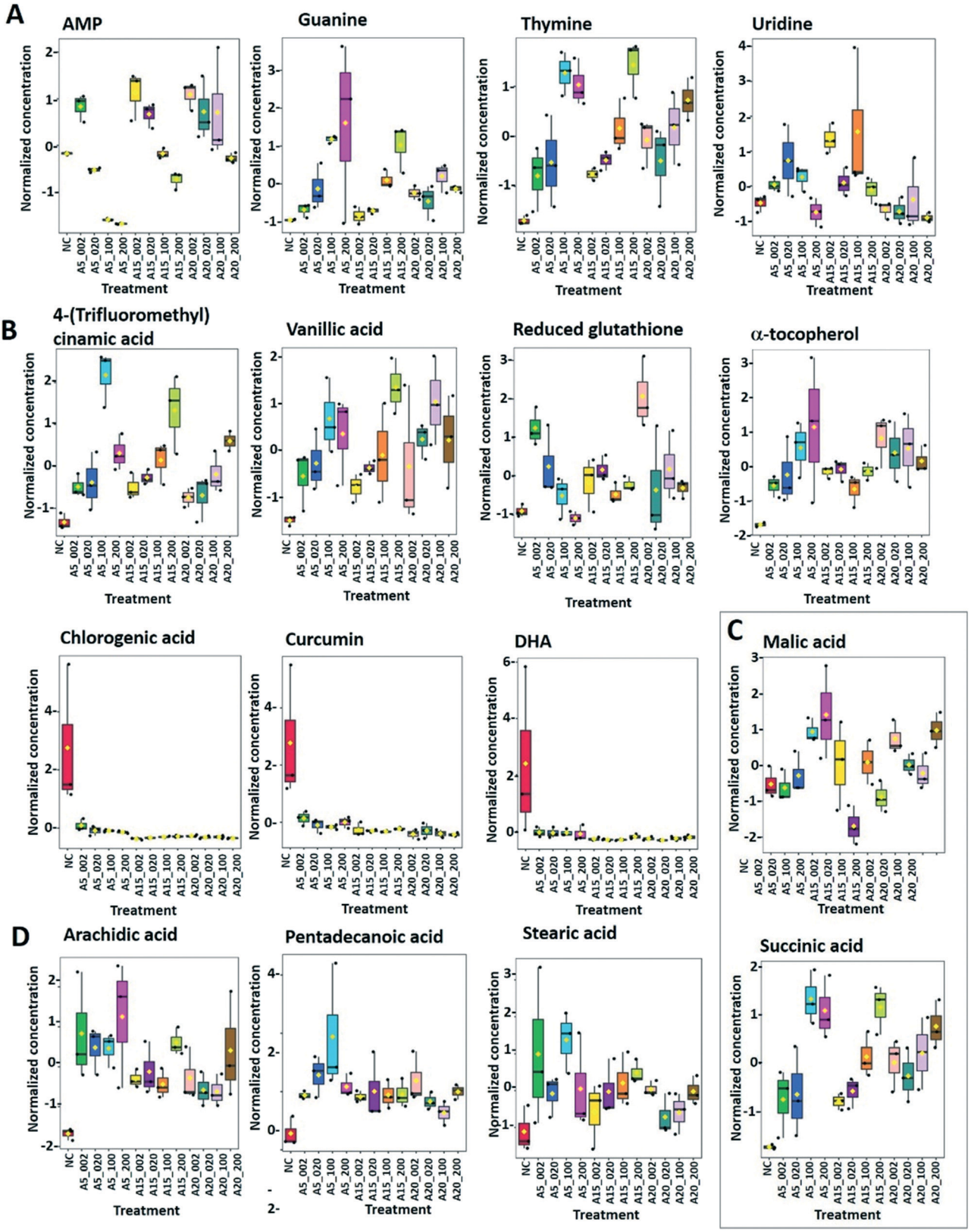

Fig. 9 Box plots of relative abundance of the (A) responsive nucleobase/tides/sides of purine and pyrimidine metabolism; (B) responsive antioxidants; (C) carboxylic acids: malic and succinic acids; (D) fatty acids; arachidic, pentadecanoic and stearic acids in *C. reinhardtii* were treated with 2–200 mg L^{-1} $nTiO_2$ with primary size of 5, 15 and 20 nm. Treatments with: 5 nm $nTiO_2$ 2 mg L^{-1} (A5_2), 20 mg L^{-1} (A5_20), 100 mg L^{-1} (A5_100) and 200 mg L^{-1} (A5_200); 15 nm $nTiO_2$ 2 mg L^{-1} (A15_2), 20 mg L^{-1} (A15_20), 100 mg L^{-1} (A15_100) and 200 mg L^{-1} (A15_200); 20 nm $nTiO_2$ (AR20): 2 mg L^{-1} (AR20_2), 20 mg L^{-1} (AR20_20), 100 mg L^{-1} (AR20_100) and 200 mg L^{-1} (AR20_200); negative control (NC). Data were row-wise normalized using probabilistic quotient normalization by reference groups, non-transformed and autoscaled.

 This journal is © The Royal Society of Chemistry 2022

Open Access Article. Published on 01 July 2022. Downloaded on 6/26/2024 11:57:25 PM. This article is licensed under a Creative Commons Attribution 3.0 Unported Licence.

consumption, *via* quenching of the ROS induced by $nTiO_2$ exposure, to prevent the damage to important cellular components.

DHA depletion could suggest depletion of ascorbic acid and/or an acceleration of the recycling and regeneration of ascorbic acid used to eliminate ROS damage and enhance stress tolerance.[85] Indeed, ascorbic acid participates in diverse cellular processes associated with photosynthetic functions and stress tolerance.[86] For example, nAg and Ag^+ induced an accumulation of ascorbic acid in *P. melhamensis*.[38]

α-Tocopherol accumulated in the all $nTiO_2$ treatments in comparison to the control (Fig. 9B). The α-tocopherol abundance increased with the A5 and A15 exposure concentrations. However, no concentration dependence was found in AR20 treatments. α-Tocopherol is a major plastid prenyllipid antioxidant able to quench and scavenge singlet oxygen ($^1O_2$), as well as scavenge superoxide ($O_2^{\bullet-}$) and lipid radicals.[87] The above observation is consistent with the literature showing an increase in the content of α- and γ-tocopherol in *C. reinhardtii* upon acclimation to chronic exposure to $Cr_2O_7^{2-}$, Cd^{2+} and Cu^{2+}.[88] However, α-tocopherol concentration decreased significantly in *C. reinhardtii* exposed to pyrazolate.[89]

The abundance of polyphenols and phenolic acids, known as antioxidants, was also altered upon $nTiO_2$ exposure. The concentrations of *vanillic* and *4-fluoro-2-methylcinnamic acids* (Fig. 9B) significantly increased in all three $nTiO_2$ material treatments in an exposure concentration dependent manner. By contrast, chlorogenic acid (CGA) and curcumin were significantly depleted in the treatments with the three $nTiO_2$. Similar depletion of these antioxidants was found in cyanobacterium *Nostoc sphaeroides* exposed to nAg and Ag^+.[90] CGA, the ester of caffeic acid and quinic acid, is known to play the role of an intermediate in lignin biosynthesis. The results indicate that the antioxidant defense system of *C. reinhardtii* was activated in $nTiO_2$ exposure, which resulted in the alteration of the abundance of the ROS-scavenging metabolites to cope with the enhanced generation of ROS. No dependence in the changes of chlorogenic acid and curcumin levels with exposure concentration or primary size of $nTiO_2$ was observed. Taken together, the above finding indicates that even at lower tested concentration of $nTiO_2$ (*i.e.* 2 mg L^{-1}) the antioxidant defense system of *C. reinhardtii* was affected, which resulted in an accumulation of the ROS-scavenging metabolites to cope with the enhanced generation of ROS (Fig. 2B). Nevertheless, the antioxidant system was overwhelmed in particularly for exposure to 100 and 200 mg L^{-1} $nTiO_2$ as can be seen by the important percentage of cells experiencing oxidative stress.

The metabolomics results were also consistent with the transcriptomic profiling. A5 at 20 mg L^{-1} down-regulated the expression of transcripts of genes involved in reduction–oxidation reaction hemostasis, such as thioredoxin (Cre16.g656600.t1.2, TY2, FC −3.37, FDR 5.89×10^{-10}) and glutathione peroxidase (Cre10.g458450.t1.3, GPX5, FC −5.07, and FDR 1.16×10^{-8}). Indeed, thioredoxin is a key molecule in the response of *C. reinhardtii* to oxidative stress induced by dissolved metals and nanoparticles.[91,92] In addition, the transcripts of genes associated with the stress response, *e.g.* "stress.abiotic.heat" such as chaperone DnaJ-domain superfamily protein were strongly up-regulated (Cre12.g488500.t1,2, FC 6.42, and FDR 1.82×10^{-8}). The transcripts of genes related to oxidative stress tolerance coding for the cysteine-rich secretory protein family[93] (Cre11.g467672.t1.1, FC 3.33, and FDR 4.96×10^{-8}, Cre06.g278160.t1.1, FC 2.83, and FDR 1.24×10^{-9}) and glycosyl hydrolase family protein[94] (Cre13.g570700.t1.3, FC 2.36, and FDR 2.63×10^{-10}) were also up-regulated. Moreover, genes involved in calcium-transporting ATPase 3, endoplasmic reticulum-type (ECA3), were also up-regulated indicating an increase of intracellular ROS production. These observations indicate an increased production of ROS induced by 20 mg L^{-1} A5 and subsequent modification of RedOx homeostasis balance in *C. reinhardtii*.

Carboxylic acid metabolism. Succinic acid concentration was significantly increased after treatments with all three $nTiO_2$. The effect was more pronounced at higher concentrations of A5, A15 or AR20 (Fig. 9C). Treatments with A5, A15 and AR20 resulted in an increase of the concentration of malic acid, another TCA cycle intermediate. However the changes in the concentrations after AR20 treatments the abundance of the malic acid was lower than control at 2 and 20 mg L^{-1} $nTiO_2$ treatments and increased at high concentrations (*i.e.*, 200 mg L^{-1}.) This finding suggests that the key cellular metabolic pathway linking carbohydrate, fatty acids, and protein metabolism, was accelerated upon $nTiO_2$ treatment probably to cope with an increase in energy production necessary for the manufacture of compounds needed to defend from $nTiO_2$ stress. Alternatively, the accumulation of TCA cycle intermediates could be also a sign of their reduced conversion. The obtained results are consistent with the finding that the concentrations of succinic and malic acids increased significantly in *P. malhamensis* and *Chlorella vulgaris*[40] exposed to Ag^+ and nAg, as well as in *C. reinhardtii* exposed to high concentration of inorganic Hg,[47] as well as the level of malic acid in *Scenedesmus obliquus* exposed to nAg.[39] By contrast, a decrease in the TCA intermediates was observed in the diatom *T. flocculosa* exposed to high Cu concentrations.[95]

Fatty acid metabolism. Among the 8 fatty acids that were measured, 3 saturated acids (*i.e.* pentadecylic acid (pentadecanoic acid, 15:0), stearic (octadecanoic acid, 18:0), arachidic (icosanoic acid, 20:0)) accumulated in cells exposed to $nTiO_2$ (Fig. 7 and 9D). However, no clear dependences on $nTiO_2$ primary size or exposure concentrations were observed. These results suggest that algae exposed to $nTiO_2$ modify the membrane fluidity to make it more tolerant to oxidation, thus preserving membrane integrity under oxidative stress conditions.[96] Indeed, saturated acids and in particular palmitic acid are known to be less prone to oxidation than other fatty acids.[96] Interestingly, changes in the abundance of unsaturated

Open Access Article. Published on 01 July 2022. Downloaded on 6/26/2024 11:57:25 PM.
This article is licensed under a Creative Commons Attribution 3.0 Unported Licence.

linoleic and linolenic acids were not significantly different from the unexposed control (all $p > 0.05$) with the exception of treatments with 2 mg L^{-1} A5, A15 and AR20. These findings suggest no significant unsaturation of the lipid membranes and alteration of integrity of lipid membranes. Indeed, this finding agrees with the relatively low percentage of cells with the affected membrane permeability found by PI in $nTiO_2$ treatments (Fig. 2C).

Similar accumulation of fatty acids has been observed in algae under toxic metal stress.[97] However, the concentrations of arachidic and stearic acids decreased in *P. malhamensis* treated with nAg.[38] nAg and Ag^+ also induced a reduction in the abundance of monounsaturated and polyunsaturated fatty acids of *Chlorella vulgaris*.[98] Plants were also shown to regulate the composition of fatty acids in the membrane to rebuild membrane integrity, as was shown for cucumber leaves exposed to nAg and Ag^+.[99]

Influence of $nTiO_2$ treatments on nutrient transport

Exposure to 20 mg L^{-1} A5 up-regulated the expression of most transcripts involved in transport, adenosine triphosphate (ATP) binding cassette (ABC) transporters, and metal transporters. Among the dysregulated ABC transporters, the multidrug resistance-associated protein 12 (Cre10.g458450.t1.3, MRP12, FC 7.38, FDR 6.40×10^{-10}) and P-loop containing nucleoside triphosphate hydrolase superfamily protein (Cre10.g444700.t1.1, FC 7.96, FDR 6.71×10^{-11}) were strongly up-regulated suggesting the involvement of the cellular mechanism in metal detoxification in algal.[100,101] Several zinc (Zn)-regulated transporters, iron (Fe)-regulated transporter-like proteins (ZIP), transporters of Fe and Zn, and Zn transporters were also up-regulated. These regulations suggest the impact of A5 on the global nutrition of the microalgal.[102] A15 and AR20 significantly dysregulated similar numbers and categories of genes (Table S10†), mostly involved in the ABC transporters and metal transporters at both concentrations.

Overall the present results revealed that 72 h exposure of green alga to $nTiO_2$ with different primary sizes altered the metabolism of amino acids, nucleotides, fatty acids, tricarboxylic acids and antioxidants, and resulted in a disturbance in a global nutrition in a concentration- and primary size-dependent way, despite the formation of micrometer-size aggregates and their sedimentation. These disturbances were consistent with the observed oxidative stress and growth inhibition observations. However, it is worth noting that the bioassays were performed at concentrations of $nTiO_2$ much higher than those typically found in the freshwater environment. As the metabolic perturbations and modes of toxic action may not be the same at a low or high exposure concentration, an extrapolation of the present observations to natural environment conditions is limited. In addition, the exposure of 72 h corresponding to chronic toxicity tests for algae was selected to gain a mechanistic understanding of the adverse outcome in an advanced time frame relative to when the physiological responses are typically assessed. However, the prolonged exposure could trigger other modes of action over time and different defense/detoxification mechanisms.[35] Despite these limitations, the study provides a unique and novel biological insight into the perturbation of the algal metabolism by $nTiO_2$ and their aggregates and potentially directs further mechanistic studies with other phytoplankton species and nanomaterials.

Conclusion

The present exploratory study provides, for the first-time, evidence of the metabolic perturbations in green alga *C. reinhardtii* exposed to increasing concentration of $nTiO_2$ with different primary sizes. The results revealed that despite the important aggregation and sedimentation, the exposure to increasing concentrations of $nTiO_2$ with primary sizes of 5, 15 and 20 nm altered the abundance of metabolites involved in various pathways corresponding to amino acid, nucleotides, fatty acid, TCA and antioxidant metabolism. Most of the responsive metabolites were common for all the treatments, however the intensity of the response and the existence or not of concentration- and nanoparticle primary size-dependences differed among the treatments. The metabolomics results correlate well with the transcriptomics and physiological results and confirmed that oxidative stress is a major toxicity mechanism for $nTiO_2$. The findings contribute to an improvement of knowledge concerning the molecular basis of these perturbations and thus to the understanding of environmental implications of one of the most used engineered nanomaterials.

Author contributions

V. I. S., W. L. and M. T. conceived and designed the study. M. T. performed the $nTiO_2$ characterization, bioassays for physiological response assessment, exposure assays for metabolomics, analyzed the physiological response data and provided interpretations, and wrote this part of the manuscript; W. L. performed exposure for transcriptomics, RNA extraction, and data processing, and wrote the transcriptomics part of the manuscript; W. W. L. performed the LC-MS measurements and data processing; V. I. S. performed analysis and interpretation of metabolomics results, wrote the metabolomics part of the manuscript, and overviewed the overall study. A. A. K. took part in the data interpretation, manuscript writing, and overviewed the overall study. All the authors critically commented and revised the manuscript. All the authors have approved the paper submission.

Conflicts of interest

The authors declare no competing interests.

 This journal is © The Royal Society of Chemistry 2022

Open Access Article. Published on 01 July 2022. Downloaded on 6/26/2024 11:57:25 PM. This article is licensed under a Creative Commons Attribution 3.0 Unported Licence.

Acknowledgements

V. I. S. and A. A. K. acknowledge the partial financial support from the Swiss National Science Foundation (grant number IZSEZ0_180186). M. T. L. acknowledges the financial support of Fondation Ernst et Lucie Schmidheiny. Dr M. Docquier and team (Genomics Platform, University of Geneva) are acknowledged for Nanostring RNA profiling and bioinformatics. Any opinions, findings, and conclusions or recommendations expressed in this material are those of the author(s) and do not necessarily reflect the views of the funding agencies.

References

1 E. Rollerova, J. Tulinska, A. Liskova, M. Kuricova, J. Kovriznych, A. Mlynarcikova, A. Kiss and S. Scsukova, Titanium dioxide nanoparticles: some aspects of toxicity/focus on the development, *Endocr. Regul.*, 2015, **49**, 97–112.

2 A. A. Keller and A. Lazareva, Predicted releases of engineered nanomaterials: From global to regional to local, *Environ. Sci. Technol. Lett.*, 2014, **1**, 65–70.

3 A. Azimzada, I. Jreije, M. Hadioui, P. Shaw, J. M. Farner and K. J. Wilkinson, Quantification and characterization of Ti-, Ce-, and Ag-nanoparticles in global surface waters and precipitation, *Environ. Sci. Technol.*, 2021, **55**, 9836–9844.

4 R. Kaegi, A. Ulrich, B. Sinnet, R. Vonbank, A. Wichser, S. Zuleeg, H. Simmler, S. Brunner, H. Vonmont, M. Burkhardt and M. Boller, Synthetic TiO_2 nanoparticle emission from exterior facades into the aquatic environment, *Environ. Pollut.*, 2008, **156**, 233–239.

5 K. Li, D. F. Xu, H. Liao, Y. Xue, M. Y. Sun, H. Su, X. J. Xiu and T. Y. Zhao, A review on the generation, discharge, distribution, environmental behavior, and toxicity (especially to microbial aggregates) of nano-TiO_2 in sewage and surface-water and related research prospects, *Sci. Total Environ.*, 2022, **824**, 153866.

6 G. V. Lowry, K. B. Gregory, S. C. Apte and J. R. Lead, Transformations of nanomaterials in the environment, *Environ. Sci. Technol.*, 2012, **46**, 6893–6899.

7 K. Kansara, S. Bolan, D. Radhakrishnan, T. Palanisami, A. A. H. Al-Muhtaseb, N. Bolan, A. Vinu, A. Kumar and A. Karakoti, A critical review on the role of abiotic factors on the transformation, environmental identity and toxicity of engineered nanomaterials in aquatic environment, *Environ. Pollut.*, 2022, **296**, 118726.

8 A. Brunelli, A. Foscari, G. Basei, G. Lusvardi, C. Bettiol, E. Semenzin, A. Marcomini and E. Badetti, Colloidal stability classification of TiO_2 nanoparticles in artificial and in natural waters by cluster analysis and a global stability index: Influence of standard and natural colloidal particles, *Sci. Total Environ.*, 2022, **829**, 154658.

9 F. Li, Z. Liang, X. Zheng, W. Zhao, M. Wu and Z. Wang, Toxicity of nano-TiO_2 on algae and the site of reactive oxygen species production, *Aquat. Toxicol.*, 2015, **158**, 1–13.

10 V. K. Sharma, Aggregation and toxicity of titanium dioxide nanoparticles in aquatic environment—a review, *J. Environ. Sci. Health, Part A: Toxic/Hazard. Subst. Environ. Eng.*, 2009, **44**, 1485–1495.

11 L. Chen, L. Zhou, Y. Liu, S. Deng, H. Wu and G. Wang, Toxicological effects of nanometer titanium dioxide (nano-TiO_2) on *Chlamydomonas reinhardtii*, *Ecotoxicol. Environ. Saf.*, 2012, **84**, 155–162.

12 Q. Abbas, B. Yousaf, H. Ullah, M. U. Ali, Y. S. Ok and J. Rinklebe, Environmental transformation and nano-toxicity of engineered nano-particles (ENPs) in aquatic and terrestrial organisms, *Crit. Rev. Environ. Sci. Technol.*, 2020, **50**, 2523–2581.

13 H. M. R. Abdel-Latif, M. A. O. Dawood, S. Menanteau-Ledouble and M. El-Matbouli, Environmental transformation of n-TiO_2 in the aquatic systems and their ecotoxicity in bivalve mollusks: A systematic review, *Ecotoxicol. Environ. Saf.*, 2020, **200**, 110776.

14 M. F. Gutierrez, A. Ale, V. Andrade, C. Bacchetta, A. Rossi and J. Cazenave, Metallic, metal oxide, and metalloid nanoparticles toxic effects on freshwater microcrustaceans: An update and basis for the use of new test species, *Water Environ. Res.*, 2021, **93**, 2505–2526.

15 Z. Luo, Z. Q. Li, Z. Xie, I. M. Sokolova, L. Song, W. Peijnenburg, M. H. Hu and Y. J. Wang, Rethinking nano-TiO_2 safety: Overview of toxic effects in humans and aquatic animals, *Small*, 2020, **16**, 2002019.

16 J. Zhao, M. Q. Lin, Z. Y. Wang, X. S. Cao and B. S. Xing, Engineered nanomaterials in the environment: Are they safe?, *Crit. Rev. Environ. Sci. Technol.*, 2021, **51**, 1443–1478.

17 A. Kahru and H.-C. Dubourguier, From ecotoxicology to nanoecotoxicology, *Toxicology*, 2010, **269**, 105–119.

18 D. Xiong, T. Fang, L. Yu, X. Sima and W. Zhu, Effects of nano-scale TiO_2, ZnO and their bulk counterparts on zebrafish: acute toxicity, oxidative stress and oxidative damage, *Sci. Total Environ.*, 2011, **409**, 1444–1452.

19 H. An, C. Ling, M. Xu, M. Hu, H. Wang, J. Liu, G. Song and J. Liu, Oxidative damage induced by nano-titanium dioxide in rats and mice: a systematic review and meta-analysis, *Biol. Trace Elem. Res.*, 2020, **194**, 184–202.

20 J. Hou, L. Wang, C. Wang, S. Zhang, H. Liu, S. Li and X. Wang, Toxicity and mechanisms of action of titanium dioxide nanoparticles in living organisms, *J. Environ. Sci.*, 2019, **75**, 40–53.

21 M. Li, W. Liu and V. I. Slaveykova, NanoTiO_2 materials mitigate mercury uptake and effects on green alga *Chlamydomonas reinhardtii* in mixture exposure, *Aquat. Toxicol.*, 2020, **224**, 105502.

22 I. M. Sadiq, S. Dalai, N. Chandrasekaran and A. Mukherjee, Ecotoxicity study of titania (TiO_2) NPs on two microalgae species: *Scenedesmus* sp. and *Chlorella* sp, *Ecotoxicol. Environ. Saf.*, 2011, **74**, 1180–1187.

23 M. Sendra, D. Sánchez-Quiles, J. Blasco, I. Moreno-Garrido, L. M. Lubián, S. Pérez-García and A. Tovar-Sánchez, Effects of TiO_2 nanoparticles and sunscreens on coastal marine

Open Access Article. Published on 01 July 2022. Downloaded on 6/26/2024 11:57:25 PM.
This article is licensed under a Creative Commons Attribution 3.0 Unported Licence.

microalgae: Ultraviolet radiation is key variable for toxicity assessment, *Environ. Int.*, 2017, **98**, 62–68.

24 D. Minetto, G. Libralato and A. Volpi Ghirardini, Ecotoxicity of engineered TiO_2 nanoparticles to saltwater organisms: An overview, *Environ. Int.*, 2014, **66**, 18–27.

25 V. Aruoja, H.-C. Dubourguier, K. Kasemets and A. Kahru, Toxicity of nanoparticles of CuO, ZnO and TiO_2 to microalgae *Pseudokirchneriella subcapitata*, *Sci. Total Environ.*, 2009, **407**, 1461–1468.

26 T. Brzicová, J. Sikorová, A. Milcová, K. Vrbová, J. Kléma, P. Pikal, Z. Lubovská, V. Philimonenko, F. Franco and J. Topinka, Nano-TiO_2 stability in medium and size as important factors of toxicity in macrophage-like cells, *Toxicol. In Vitro*, 2019, **54**, 178–188.

27 X. He, C. Xie, Y. Ma, L. Wang, X. He, W. Shi, X. Liu, Y. Liu and Z. Zhang, Size-dependent toxicity of ThO_2 nanoparticles to green algae *Chlorella pyrenoidosa*, *Aquat. Toxicol.*, 2019, **209**, 113–120.

28 L. Clément, C. Hurel and N. Marmier, Toxicity of TiO_2 nanoparticles to cladocerans, algae, rotifers and plants – Effects of size and crystalline structure, *Chemosphere*, 2013, **90**, 1083–1090.

29 A. Menard, D. Drobne and A. Jemec, Ecotoxicity of nanosized TiO2. Review of in vivo data, *Environ. Pollut.*, 2011, **159**, 677–684.

30 M. Kulasza and L. Skuza, Changes of gene expression patterns from aquatic organisms exposed to metal nanoparticles, *Int. J. Environ. Res. Public Health*, 2021, **18**, 8361.

31 M. Revel, A. Chatel and C. Mouneyrac, Omics tools: New challenges in aquatic nanotoxicology?, *Aquat. Toxicol.*, 2017, **193**, 72–85.

32 M. Mortimer, Y. Wang and P. A. Holden, Molecular mechanisms of nanomaterial-bacterial interactions revealed by omics-The role of nanomaterial effect level, *Front. Bioeng. Biotechnol.*, 2021, **9**, 683520.

33 S. Majumdar and A. A. Keller, Omics to address the opportunities and challenges of nanotechnology in agriculture, *Crit. Rev. Environ. Sci. Technol.*, 2021, **51**, 2595–2636.

34 H. M. Kim and J. S. Kang, Metabolomic studies for the evaluation of toxicity induced by environmental toxicants on model organisms, *Metabolites*, 2021, **11**, 485.

35 G. T. Ankley, R. S. Bennett, R. J. Erickson, D. J. Hoff, M. W. Hornung, R. D. Johnson, D. R. Mount, J. W. Nichols, C. L. Russom, P. K. Schmieder, J. A. Serrrano, J. E. Tietge and D. L. Villeneuve, Adverse outcome pathways: a conceptual framework to support ecotoxicology research and risk assessment, *Environ. Toxicol. Chem.*, 2010, **29**, 730–741.

36 E. Morel, I. Jreije, V. Tetreault, C. Hauser, W. Zerges and K. J. Wilkinson, Biological impacts of Ce nanoparticles with different surface coatings as revealed by RNA-Seq in *Chlamydomonas reinhardtii*, *Nanoimpact*, 2020, **19**, 100228.

37 S. Chen, N. Shi, M. Huang, X. Tan, X. Yan, A. Wang, Y. Huang, R. Ji, D. Zhou, Y.-G. Zhu, A. A. Keller, J. L. Gardea-Torresdey, J. C. White and L. Zhao, MoS_2 nanosheets–cyanobacteria interaction: Reprogrammed carbon and nitrogen metabolism, *ACS Nano*, 2021, **15**, 16344–16356.

38 W. Liu, S. Majumdar, W. Li, A. A. Keller and V. I. Slaveykova, Metabolomics for early detection of stress in freshwater alga *Poterioochromonas malhamensis* exposed to silver nanoparticles, *Sci. Rep.*, 2020, **10**, 1–13.

39 P. Wang, B. Zhang, H. Zhang, Y. L. He, C. N. Ong and J. Yang, Metabolites change of *Scenedesmus obliquus* exerted by AgNPs, *J. Environ. Sci.*, 2019, **76**, 310–318.

40 R. Qu, Q. Xie, J. Tian, M. Zhou and F. Ge, Metabolomics reveals the inhibition on phosphorus assimilation in *Chlorella vulgaris* F1068 exposed to AgNPs, *Sci. Total Environ.*, 2021, **770**, 145362.

41 J. L. Zhang, Z. P. Zhou, Y. Pei, Q. Q. Xiang, X. X. Chang, J. Ling, D. Shea and L. Q. Chen, Metabolic profiling of silver nanoparticle toxicity in *Microcystis aeruginosa*, *Environ. Sci.: Nano*, 2018, **5**, 2519–2530.

42 D. F. Simon, R. F. Domingos, C. Hauser, C. M. Hutchins, W. Zerges and K. J. Wilkinson, Transcriptome sequencing (RNA-seq) analysis of the effects of metal nanoparticle exposure on the transcriptome of *Chlamydomonas reinhardtii*, *Appl. Environ. Microbiol.*, 2013, **79**, 4774–4785.

43 M. Li and V. I. Slaveykova, Kinetic aspects of the interactions between TiO_2 nanoparticles, mercury and the green alga *Chlamydomonas reinhardtii*, *Environments*, 2022, **9**, 44.

44 A. Kahru and A. Ivask, Mapping the Ddawn of nanoecotoxicological research, *Acc. Chem. Res.*, 2013, **46**, 823–833.

45 E. H. Harris, *The Chlamydomonas sourcebook: a comprehensive guide to biology and laboratory use*, Elsevier, 2013.

46 G. Cheloni, C. Cosio and V. I. Slaveykova, Antagonistic and synergistic effects of light irradiation on the effects of copper on *Chlamydomonas reinhardtii*, *Aquat. Toxicol.*, 2014, **155**, 275–282.

47 V. I. Slaveykova, S. Majumdar, N. Regier, W. Li and A. A. Keller, Metabolomic responses of green alga *Chlamydomonas reinhardtii* exposed to sublethal concentrations of inorganic and methylmercury, *Environ. Sci. Technol.*, 2021, **55**, 3876–3887.

48 Y. Huang, W. Li, A. S. Minakova, T. Anumol and A. A. Keller, Quantitative analysis of changes in amino acids levels for cucumber (*Cucumis sativus*) exposed to nano copper, *NanoImpact*, 2018, **12**, 9–17.

49 Y. Huang, A. S. Adeleye, L. Zhao, A. S. Minakova, T. Anumol and A. A. Keller, Antioxidant response of cucumber (*Cucumis sativus)* exposed to nano copper pesticide: Quantitative determination via LC-MS/MS, *Food Chem.*, 2019, **270**, 47–52.

50 S. Majumdar, L. Pagano, J. A. Wohlschlegel, M. Villani, A. Zappettini, J. C. White and A. A. Keller, Proteomic, gene and metabolite characterization reveal the uptake and toxicity mechanisms of cadmium sulfide quantum dots in soybean plants, *Environ. Sci.: Nano*, 2019, **6**, 3010–3026.

 This journal is © The Royal Society of Chemistry 2022

Open Access Article. Published on 01 July 2022. Downloaded on 6/26/2024 11:57:25 PM.
This article is licensed under a Creative Commons Attribution 3.0 Unported Licence.

51 Z. Pang, J. Chong, G. Zhou, D. A. de Lima Morais, L. Chang, M. Barrette, C. Gauthier, P.-É. Jacques, S. Li and J. Xia, MetaboAnalyst 5.0: narrowing the gap between raw spectra and functional insights, *Nucleic Acids Res.*, 2021, **49**, W388–W396.

52 Y. Jung, Y. G. Ahn, H. K. Kim, B. C. Moon, A. Y. Lee, D. H. Ryu and G. S. Hwang, Characterization of dandelion species using 1H NMR- and GC-MS-based metabolite profiling, *Analyst*, 2011, **136**, 4222–4231.

53 J. Chong, D. S. Wishart and J. Xia, Using MetaboAnalyst 4.0 for Comprehensive and Integrative Metabolomics Data Analysis, *Curr. Protoc. Bioinf.*, 2019, **68**, e86.

54 J. Xia and D. S. Wishart, Web-based inference of biological patterns, functions and pathways from metabolomic data using MetaboAnalyst, *Nat. Protoc.*, 2011, **6**, 743.

55 J. Xia and D. S. Wishart, MSEA: a web-based tool to identify biologically meaningful patterns in quantitative metabolomic data, *Nucleic Acids Res.*, 2010, **38**, W71–W77.

56 R. Beauvais-Flück, V. I. Slaveykova and C. Cosio, Cellular toxicity pathways of inorganic and methyl mercury in the green microalga *Chlamydomonas reinhardtii*, *Sci. Rep.*, 2017, **7**, 1–12.

57 O. Thimm, O. Bläsing, Y. Gibon, A. Nagel, S. Meyer, P. Krüger, J. Selbig, L. A. Müller, S. Y. Rhee and M. Stitt, MAPMAN: a user-driven tool to display genomics data sets onto diagrams of metabolic pathways and other biological processes, *Plant J.*, 2004, **37**, 914–939.

58 R. Beauvais-Flück, V. I. Slaveykova, S. Ulf and C. Cosio, Towards early-warning gene signature of *Chlamydomonas reinhardtii* exposed to Hg-containing complex media, *Aquat. Toxicol.*, 2019, **214**, 105259.

59 P. Dranguet, C. Cosio, S. Le Faucheur, R. Beauvais-Flück, A. Freiburghaus, I. A. Worms, B. Petit, N. Civic, M. Docquier and V. I. Slaveykova, Transcriptomic approach for assessment of the impact on microalga and macrophyte of in-situ exposure in river sites contaminated by chlor-alkali plant effluents, *Water Res.*, 2017, **121**, 86–94.

60 G. K. Geiss, R. E. Bumgarner, B. Birditt, T. Dahl, N. Dowidar, D. L. Dunaway, H. P. Fell, S. Ferree, R. D. George and T. Grogan, Direct multiplexed measurement of gene expression with color-coded probe pairs, *Nat. Biotechnol.*, 2008, **26**, 317–325.

61 J. Vandesompele, K. De Preter, F. Pattyn, B. Poppe, N. Van Roy, A. De Paepe and F. Speleman, Accurate normalization of real-time quantitative RT-PCR data by geometric averaging of multiple internal control genes, *Genome Biol.*, 2002, **3**, 1–12.

62 Y. Hochberg and Y. Benjamini, More powerful procedures for multiple significance testing, *Stat. Med.*, 1990, **9**, 811–818.

63 A. A. Keller, H. Wang, D. Zhou, H. S. Lenihan, G. Cherr, B. J. Cardinale, R. Miller and Z. Ji, Stability and aggregation of metal oxide nanoparticles in natural aqueous matrices, *Environ. Sci. Technol.*, 2010, **44**, 1962–1967.

64 J. Wang, Y. Sun, M. Yu, X. Lu, S. Komarneni and C. Yang, Emulsions stabilized by highly hydrophilic TiO_2 nanoparticles via van der Waals attraction, *J. Colloid Interface Sci.*, 2021, **589**, 378–387.

65 I. M. Nadeem, L. Hargreaves, G. T. Harrison, H. Idriss, A. L. Shluger and G. Thornton, Carboxylate adsorption on rutile TiO_2 (100): Role of Coulomb repulsion, relaxation, and steric hindrance, *J. Phys. Chem. C*, 2021, **25**, 13770–13779.

66 O. Vallon and M. H. Spalding, in *The Chlamydomonas Sourcebook*, ed. E. H. Harris, D. B. Stern and G. B. Witman, Academic Press, London, 2nd edn, 2009, pp. 115–158, DOI: 10.1016/B978-0-12-370873-1.00012-5.

67 N. L. Taylor, J. L. Heazlewood, D. A. Day and A. H. Millar, Lipoic acid-dependent oxidative catabolism of alpha-keto acids in mitochondria provides evidence for branched-chain amino acid catabolism in Arabidopsis, *Plant Physiol.*, 2004, **134**, 838–848.

68 B. G. Forde and P. J. Lea, Glutamate in plants: metabolism, regulation, and signalling, *J. Exp. Bot.*, 2007, **58**, 2339–2358.

69 M. Wirtz and M. Droux, Synthesis of the sulfur amino acids: Cysteine and methionine, *Photosynth. Res.*, 2006, **86**, 345–362.

70 K. Lameka, M. D. Farwell and M. Ichise, in *Handbook of Clinical Neurology*, ed. J. C. Masdeu and R. G. González, Elsevier, 2016, vol. 135, pp. 209–227.

71 H. Less and G. Galili, Principal transcriptional programs regulating plant amino acid metabolism in response to abiotic stresses, *Plant Physiol.*, 2008, **147**, 316–330.

72 M. A. Lieberman and R. Ricer, *Brs Biochemistry, Molecular Biology, And Genetics*, Wolters Kluwer, Lippincott Williams and Wilkins, 6th edn, 2013.

73 T. M. Hildebrandt, A. Nunes Nesi, W. L. Araújo and H.-P. Braun, Amino acid catabolism in plants, *Mol. Plant*, 2015, **8**, 1563–1579.

74 J. Matysik, Alia, B. Bhalu and P. Mohanty, Molecular mechanisms of quenching of reactive oxygen species by proline under stress in plants, *Curr. Sci.*, 2002, **82**, 525–532.

75 S. S. Sharma and K.-J. Dietz, The significance of amino acids and amino acid-derived molecules in plant responses and adaptation to heavy metal stress, *J. Exp. Bot.*, 2006, **57**, 711–726.

76 B. Sekula, M. Ruszkowski and Z. Dauter, Structural analysis of phosphoserine aminotransferase (Isoform 1) from *Arabidopsis thaliana*–the enzyme involved in the phosphorylated pathway of serine biosynthesis, *Front. Plant Sci.*, 2018, **9**, 876.

77 H. Andre'O, C. Bless, P. Macedo, S. P. Chatterjee, B. K. Singh, C. Gilvarg and T. Leustek, Biosynthesis of lysine in plants: evidence for a variant of the known bacterial pathways, *Biochim. Biophys. Acta, Gen. Subj.*, 2005, **1721**, 27–36.

78 C. Carrie, M. W. Murcha, A. H. Millar, S. M. Smith and J. Whelan, Nine 3-ketoacyl-CoA thiolases (KATs) and acetoacetyl-CoA thiolases (ACATs) encoded by five genes in Arabidopsis thaliana are targeted either to peroxisomes or cytosol but not to mitochondria, *Plant Mol. Biol.*, 2007, **63**, 97–108.

Open Access Article. Published on 01 July 2022. Downloaded on 6/26/2024 11:57:25 PM.
This article is licensed under a Creative Commons Attribution 3.0 Unported Licence.

79 C. Han, C. Ren, T. Zhi, Z. Zhou, Y. Liu, F. Chen, W. Peng and D. Xie, Disruption of fumarylacetoacetate hydrolase causes spontaneous cell death under short-day conditions in Arabidopsis, *Plant Physiol.*, 2013, **162**, 1956–1964.

80 N. V. Bhagavan and C.-E. Ha, Nucleotide Metabolism, in *Essentials of Medical Biochemistry*, ed. N. V. Bhagavan and C.-E. Ha, Imprint: Academic Press, 2015, p. 752, vol. eBook ISBN: 9780124166974.

81 C. H. Foyer and G. Noctor, Ascorbate and glutathione: The heart of the redox hub, *Plant Physiol.*, 2011, **155**, 2–18.

82 A. Jamers, R. Blust, W. De Coen, J. L. Griffin and O. A. H. Jones, An omics based assessment of cadmium toxicity in the green alga *Chlamydomonas reinhardtii*, *Aquat. Toxicol.*, 2013, **126**, 355–364.

83 T. L. Stoiber, M. M. Shafer and D. E. Armstrong, Differential effects of copper and cadmium exposure on toxicity endpoints and gene expression in *Chlamydomonas reinhardtii*, *Environ. Toxicol. Chem.*, 2010, **29**, 191–200.

84 A. Jamers, R. Blust, W. De Coen, J. L. Griffin and O. A. Jones, Copper toxicity in the microalga *Chlamydomonas reinhardtii*: an integrated approach, *BioMetals*, 2013, **26**, 731–740.

85 M. Xiao, Z. Li, L. Zhu, J. Wang, B. Zhang, F. Zheng, B. Zhao, H. Zhang, Y. Wang and Z. Zhang, The multipleroles of ascorbate in the abiotic stress response of plants: Antioxidant, cofactor, and regulator, *Front. Plant Sci.*, 2021, **12**, 598173.

86 N. Gest, H. Gautier and R. Stevens, Ascorbate as seen through plant evolution: the rise of a successful molecule?, *J. Exp. Bot.*, 2012, **64**, 33–53.

87 B. Nowicka and J. Kruk, Plastoquinol is more active than α-tocopherol in singlet oxygen scavenging during high light stress of *Chlamydomonas reinhardtii*, *Biochim. Biophys. Acta, Bioenerg.*, 2012, **1817**, 389–394.

88 B. Nowicka, B. Pluciński, P. Kuczyńska and J. Kruk, Physiological characterization of *Chlamydomonas reinhardtii* acclimated to chronic stress induced by Ag, Cd, Cr, Cu and Hg ions, *Ecotoxicol. Environ. Saf.*, 2016, **130**, 133–145.

89 B. Nowicka, T. Fesenko, J. Walczak and J. Kruk, The inhibitor-evoked shortage of tocopherol and plastoquinol is compensated by other antioxidant mechanisms in *Chlamydomonas reinhardtii* exposed to toxic concentrations of cadmium and chromium ions, *Ecotoxicol. Environ. Saf.*, 2020, **191**, 110241.

90 M. Huang, A. A. Keller, X. Wang, L. Tian, B. Wu, R. Ji and L. Zhao, Low concentrations of silver nanoparticles and silver ions perturb the antioxidant defense system and nitrogen metabolism in N_2-fixing cyanobacteria, *Environ. Sci. Technol.*, 2020, **54**, 15996–16005.

91 S. D. Lemaire, B. Guillon, P. Le Maréchal, E. Keryer, M. Miginiac-Maslow and P. Decottignies, New thioredoxin targets in the unicellular photosynthetic eukaryote *Chlamydomonas reinhardtii*, *Proc. Natl. Acad. Sci. U. S. A.*, 2004, **101**, 7475–7480.

92 F. Montrichard, F. Alkhalfioui, H. Yano, W. H. Vensel, W. J. Hurkman and B. B. Buchanan, Thioredoxin targets in plants: the first 30 years, *J. Proteomics*, 2009, **72**, 452–474.

93 X. Liu, H. Zhang, H. Jiao, L. Li, X. Qiao, M. R. Fabrice, J. Wu and S. Zhang, Expansion and evolutionary patterns of cysteine-rich peptides in plants, *BMC Genomics*, 2017, **18**, 1–14.

94 W. Chen, X. Jiang and Q. Yang, Glycoside hydrolase family 18 chitinases: The known and the unknown, *Biotechnol. Adv.*, 2020, **43**, 107553.

95 S. Gonçalves, M. Kahlert, S. F. P. Almeida and E. Figueira, Assessing Cu impacts on freshwater diatoms: biochemical and metabolomic responses of *Tabellaria flocculosa* (Roth) Kützing, *Sci. Total Environ.*, 2018, **625**, 1234–1246.

96 R. G. Upchurch, Fatty acid unsaturation, mobilization, and regulation in the response of plants to stress, *Biotechnol. Lett.*, 2008, **30**, 967–977.

97 E. Pinto, T. C. S. Sigaud-kutner, M. A. S. Leitão, O. K. Okamoto, D. Morse and P. Colepicolo, Heavy metal-induced ooxidative stress in algae, *J. Phycol.*, 2003, **39**, 1008–1018.

98 M. Behzadi Tayemeh, M. Esmailbeigi, I. Shirdel, H. S. Joo, S. A. Johari, A. Banan, H. Nourani, H. Mashhadi, M. J. Jami and M. Tabarrok, Perturbation of fatty acid composition, pigments, and growth indices of Chlorella vulgaris in response to silver ions and nanoparticles: A new holistic understanding of hidden ecotoxicological aspect of pollutants, *Chemosphere*, 2020, **238**, 124576.

99 H. Zhang, W. Du, J. R. Peralta-Videa, J. L. Gardea-Torresdey, J. C. White, A. Keller, H. Guo, R. Ji and L. Zhao, Metabolomics reveals how cucumber (*Cucumis sativus*) reprograms metabolites to cope with silver ions and silver nanoparticle-induced oxidative stress, *Environ. Sci. Technol.*, 2018, **52**, 8016–8026.

100 A. Georgantzopoulou, S. Cambier, T. Serchi, M. Kruszewski, Y. L. Balachandran, P. Grysan, J.-N. Audinot, J. Ziebel, C. Guignard and A. C. Gutleb, Inhibition of multixenobiotic resistance transporters (MXR) by silver nanoparticles and ions in vitro and in *Daphnia magna*, *Sci. Total Environ.*, 2016, **569**, 681–689.

101 J. Park, W. Y. Song, D. Ko, Y. Eom, T. H. Hansen, M. Schiller, T. G. Lee, E. Martinoia and Y. Lee, The phytochelatin transporters AtABCC1 and AtABCC2 mediate tolerance to cadmium and mercury, *Plant J.*, 2012, **69**, 278–288.

102 M. L. Guerinot, The ZIP family of metal transporters, *Biochim. Biophys. Acta, Biomembr.*, 2000, **1465**, 190–198.

 This journal is © The Royal Society of Chemistry 2022